ISSN 0255-7193

CLAY RESEARCH

Vol. 35, No. 2

December, 2016

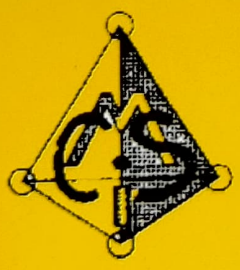

IOS Press

Overseas distribution
IOS Press, The Netherlands

THE CLAY MINERALS SOCIETY OF INDIA
Division of Soil Science and
Agricultural Chemistry
Indian Agricultural Research Institute
New Delhi-110 012, India

Overseas subscribers may send their queries to IOS Press, Nieuwe Hemweg 6B, 1013 BG Amsterdam, The Netherlands, orders@iospress.in:
URL: http://www.iospress.nl

THE CLAY MINERALS SOCIETY OF INDIA

(Registered under Act XXI of 1860)
Registration No. S/13028 of 1982

COUNCIL FOR 2016

President	:	Dr. S.K. Singh
Vice Presidents	:	Dr. D.C. Nayak
		Dr. Nayan Ahmed
Secretary	:	Dr. S.K. Mahapatra
Joint Secretaries	:	Dr. Gautam Goswami
		Dr. Sudarshan Dutta
Treasurer	:	Dr. Jaya N. Surya
Chief Editor	:	Dr. S.C. Datta
Editors	:	Dr. K. M. Manjaih
		Dr. S.K. Roy
		Dr. P. Chandran
Councilor	:	East zone : Dr. A.K. Sahoo, Dr. Siladitya Bandopadhyay
Councilor	:	West zone : Dr. A.L. Pharande, Dr. Vilas kharche
Councilor	:	North zone : Dr. U.K Maurya, Dr. B.N. Ghosh
Councilor	:	South zone : Dr. K.S. Anil Kumar, Dr. Chandrakala M.
Councilor	:	Central zone : Dr. P. Chandran, Dr. Tapan Adhikari
Past Presidents	:	Dr S.K. Mukherjee, Dr K.V. Raman, Dr S.K. Ghosh, Dr. D.K. Pal, Dr. Dipak Sarkar

EDITORIAL BOARD

International Consulting Editor	:	Dr. S.R. Krishnamurti Gummuluru Adjunct Associate Professor, CERAR, University of South Australia, Canada Dr. Sridhar Komarneni Adjunct Professor of Civil and Environmental Engineering & Editor-in-Chief, J. Porous Materials, USA

Annual Institutional Subscription Rates Inclusive of Air Mail and Handling Charges :

Subscription Rates (Year 2011)	Indian (INR)	Overseas (USD)
Print + online access	Rs. 1,800.00	$ 350.00
Online access	Rs. 600.00	$ 150.00
Print	Rs. 1,200.00	$ 200.00

All payments should be sent to **"The Clay Minerals Society of India"** Division of Soil Science and Agricultural Chemistry, I.A.R.I., New Delhi-110 012

Clay Research, Vol. 35, No. 2, pp. 55-60 (2016)

Refinement of Low-Grade Kaolin by Microbial Removal of Iron Compounds

MOHAMMAD R. SAERI[1], SASAN OTROJ [1], MOHAMMAD H. SALEHI[2], ASIYEH ALIDOOSTI-SHAHRAKI [3] AND IBRAHIM SHARIFI[1*]

[1]Department of Material Engineering, Faculty of Engineering, Shahrekord University, Shahrekord, Iran,
[2]Department of Soil Science, Faculty of Agriculture, Shahrekord University, Shahrekord, Iran,
[3]Department of Geology, Faculty of Science, The University of Isfahan, Isfahan, Iran.

Abstract–*The objective of this study was to evaluate the effects of time on feeding a micro-organism by using maltose as a source of carbon and nitrogen in order to remove iron impurities from kaolin. Therefore, kaolin sample was provided from a deposit located in Abadeh, Fars Province, Iran. Since it contains high amount of iron oxides (6.1% Fe_2O_3), it is not suitable for sanitary manufacturing of ceramic body. X-ray diffraction (XRD) and X-ray fluorescence spectroscopy (XRF) techniques were used in order to determine absolute amount of characterization and chemical contents of samples before and after leaching respectively. X Atomic absorption spectroscopy (AAS) analysis was performed to determine concentration of iron ions existing in aqueous solution of samples. Statistical analysis was completed by one Way ANOVA. Differences were considered significant if $P<0.05$. Scanning Electron Microscopic (SEM) equipped with EDS analysis of the sample was performed to get an atomic level chemical composition of the impurity minerals after bioleaching. According to AAS and XRD measurements, the Abadeh kaolin sample which was taken for this study has different types of impurity mineral species. The major iron impurity mineral species is hematite along with pyrite as minor secondary mineral. The results of EDS analysis confirmed that bioleaching had not made an important change in chemical composition of the samples. Statistical analysis showed that differences between all groups were significant ($P<0.05$). Regarding the decrease in iron impurity, the processed kaolin can be a suitable candidate to be used in ceramic and porcelain industries.*

Key words *:* Kaolin, microorganism, Iron, Leaching, Ceramic.

Introduction

The most commonly used clay in ceramics manufacturing is kaolin which contain large proportions of mineral kaolinite generally, however, kaolin can contain substantial amounts of other clay minerals. Kaolin, $Al_2O_3.2SiO_2.2H_2O$, is an essential resource in porcelain, pottery, paper, pigment, and filter manufacturing (Adamis and Williams 2005; Adefila 2012). Low-quality kaolin's are also used as fillers in a wide range of ceramic products including brick, pipes, and tiles (Zegeye *et al.,* 2013).

Iron is regularly a most important impurity element, substituted for aluminum in silicate structures or connected in oxide and hydroxide compounds, which impact its refractoriness and whiteness (Mockovèiaková *et al.,* 2008). Refractory clays are dominantly composed of kaolins with low levels of iron, alkali, and alkaline earth cations. High levels of such metals would reduce the fusion point. Naturally, Kaolin has different levels of iron impurities that could affect its quality such as whiteness and fusion point (Stucki, Goodman, and Schwertmann 1988).

***Corresponding author email :** saeri_mohammad@yahoo.com

Much greater amount of iron impurity in kaolin clay can cause lower commercial value. Many physical and chemical methods such as froth flotation, gravity separation, magnetic separation, reductive roasting, and acid treatment have already been used to improve the purity of kaolin minerals. Physical methods are often not efficient enough to remove impurities because absorption of iron in kaolin is strong or because iron has a complex form (He, Huang, and Chen 2011). Although leaching as a chemical approach possesses high efficiency, this method is costly to implement and environmentally hazardous.On the other hand, another approach that has recently received considerable attention is the use of iron-reducing micro-organisms.It is found that iron oxides present as impurities in kaolin can be efficiently removed by leaching and various micro-organism. Different types of micro-organisms can reduce iron from ferric (Fe (III)) to ferrous (Fe (II)), following this process ferrous iron is dissolved in the water and therefore the amount of impurities in kaolin is decreased. Some of these micro-organisms are *Bacillus spp., Geobacter metallireducens,* and *Shewanella species* or mixed iron reducing bacteria (IRB)(Cooper et al. 2005; Zegeye et al. 2013).

The iron removal by means of culture solutions containing soluble microbial metabolites can be very efficient. An important part of the soil microbial community are IRB, and most of these bacteria are facultative anaerobes. Consequently, if oxygen is available, they will consume it for their growth while also keeping on their capability of growth under anaerobic conditions since these bacteria are chemoheterotrophic (consume organic compounds as the source of energy) and facultative anaerobes. The bacteria community on the surface of soil is much higher than depth of soil, especially if soil is rich in organic compound on surface level. Some IRB such as *Shewanella purefaciens* can use Fe (III), Mn (IV), NO_3, NO_2, S_2O_3 and others in anaerobic respiration (Gonzalez and Delcruiz 2006; Javaherdashti 2008; Williamson *et al.* 2013).

The present paper contains some data about experiments intended to evaluate the effects of time on feeding a micro-organism by using maltose as a source of carbon and nitrogen in removing iron impurities from kaolin.

Materials and Methods

Kaolin samples

Kaolin sample was provided from a deposit located in Abadeh, Fars Province, Iran. This deposit is not suitable for sanitary-ware manufacturing of ceramic body since it contains high level of iron oxides (6.1% Fe_2O_3). Kaolin sample was collected from moist clay in active mines naturally, wrapped with plastic, and sent to the laboratory immediately. Subsequently, the sample was placed in an N_2-filled serum bottles. The nitrogen gas was used as respiration of IRB micro-organism.

Microorganisms and culture media

After preparing the soil and crushing by Jar Mill, it was passed through a sieve to get fine-grained.According to Shelobolina group work (Shelobolina, Pickering, and Lovley 2005), the culture medium must have an anaerobic environment of N_2/CO_2, However, there was no room for presence of air virtually due to the large amount of required raw material in experimental work. As a result, mixed medium culture included: 55 g kaolin, 300 ml tap water, 21 g maltose (Maximum 5%) in 500ml serum bottles. Subsequently, by purging the head space of serum bottles with nitrogen gas and sealing with a butyl rubber stopper, anaerobic condition was provided to the micro-organism culture. The bottles were then incubated in Bain-marie bath at 30!. Fermentative gases formed during cultivation and were collected with a 30 ml syringe installed on each bottle. These experiment were carried out

for 3 times. Thirty ml of the kaolin sample was inoculated into 270 ml of fresh medium when color of the culture medium changed from pink to white. After this process was repeated 10 times, the acclimated mixed culture broth was used as the inoculum source for subsequent experiments. Afterwards each iteration of the above analysis of iron content by AAS system were measured. Consequently, microbial removal of iron content was started by using 120 ml serum bottles. The bottles were charged with 10 g of dry kaolin, 50 ml of tap water, 0.4 g of maltose, and 1 ml of mixed culture broth. Incubation methods were performed in the same manner as described in the cultivation of iron-reducing micro-organisms. The effect of inoculation was evaluated by comparing the removal efficiencies of Fe (III) impurities with and without inoculation of the mixed iron-reducing culture.

Characterization

X-ray fluorescence spectroscopy (XRF) analysis was used by ARL 8410 instrument; tube anode, Rh, and 60 kV to determine kaolin composition and especially its iron contents. In order to determine the amount of removable iron by leaching process, 20 ml of nitric acid (7.5 M) was added to the 1g kaolin initially and then it was aged for 16 hours to break up iron content of the soil in an acid solution. Subsequently, it was heated by oven for 30min at 120 !. Finally, the mixture was passed through the filter paper and iron content was determined by AAS instrument. Moreover, FESEM study was carried out in a TESCAN field emission type scanning electron microscope at 10 kV.

Result and Discussion

Geology

Based on mineralogy aspect, kaolin deposits of Iran can be divided into two types:

Alteration or hydrothermal type deposits. This type of kaolin has a weighty amounts of quartz and sometimes alunite. Therefore, the percentage of silicon oxide is more than 60% and aluminum oxide is less than 24%. These kaolin minerals are usually due to Tertiary volcanic activities in Azerbaijan, Alborz, and east of Iran (Ghorbani 2013).

Sedimentary-type deposits. Sedimentary-type deposits are products of erosion and alteration carried out on rocks which were rich in feldspar. In these types, silicon oxide content does not go beyond 60%, however, the amount of aluminum oxide can be changed from 25% to 49%. Iron minerals such as hematite are mostly seen in their paragenesis. The anatase form of titanium can be seen in this kaolin occasionally. These deposits are fire resistant and have high plasticity (Ghorbani 2013).

Abadeh kaolin is one of the most important and famous clay deposits in this group technically. These deposits are products of erosion and sedimentation of volcanic rocks. As a geological aspect, Abadeh kaolin was owned by Late Paleozoic–Early Mesozoic typically, however, some of them were formed in Cretaceous (Ghorbani 2013).

Structural analysis

Chemical analysis of kaolin samples has been completed by XRF method. The results revealed

Table 1. *XRF data of the Abadeh kaolin before microbial treatment.*

	Weight percentage %	Standard error %
SiO_2	57.9	0.2
Al_2O_3	29.1	0.2
Fe_2O_3	6.1	0.1
K_2O	2.1	0.07
Na_2O	1.5	0.06
TiO_2	1.1	0.05
CaO	0.54	0.03
MgO	0.50	0.03
SO_3	0.25	0.02
Trace compound	0.91	

high iron impurity (~6.1% Fe_2O_3) and presence of few other impurities such as K_2O, Na_2O, and TiO_2 (Table 1).

XRD is the most direct and precise analytical technique for determining the presence and absolute amounts of minerals species in a sample. The XRD patterns of kaolin sample before and after bioleaching are shown (Figures 1 and 2). According to the results of XRD analysis, Abadeh clay phases included kaolinite, quartz, illite, hematite and pyrite phases. Amount of pyrite and hematite before and after bioleaching indicated valuable changes. As acknowledged in XRD analysis, the peak intensity in 29° of spectra

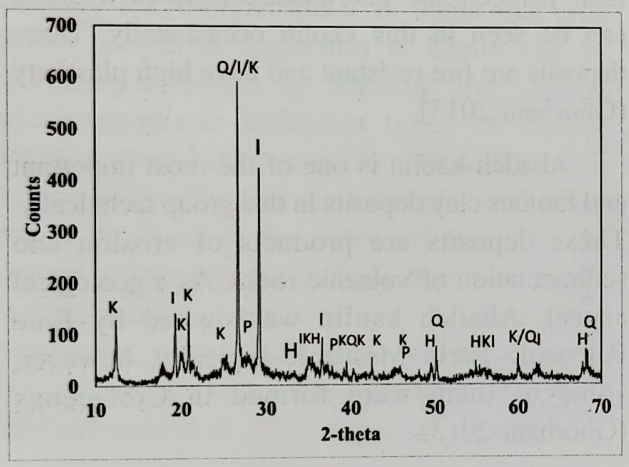

Fig. 1. *Symbolic X-ray diffraction patterns of Abadeh kaolin sample before microbial treatment. K = kaolinite; I = Illite; Q = quartz; H = hematite and P = pyrite.*

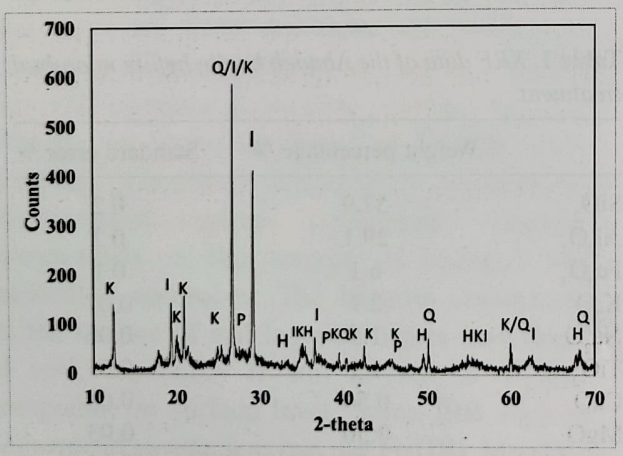

Fig. 2. *Symbolic X-ray diffraction patterns of Abadeh kaolin sample After its microbial treatment for 3 weeks.*

decreased as iron content reduced in form of pyrite from kaolin clay. Furthermore, hematite related peaks decreased as a result of microbial bioleaching. Semi-quantitative phase analysis before and after bioleaching by Reference **Fig. 1** Intensity Ratio (RIR) method for samples can be find in Table 2.

Table 2. *XRD analysis of Abadeh kaolin before and after microbial bioleaching.*

	Before bioleaching (±1%)	After bioleaching (±1%)
Kaolinite	33.7	37.1
Illite	37.8	38.0
Quartz	22.3	21.4
Hematite	4.4	3.2
Pyrite	1.8	0.3

The high amount of illite content shows that the sedimentary deposition can be occurred to kaolin clay (Ghorbani 2013). Rock weathering regularly started by acidic agents. Alkalis minerals such as illite can be dissolved under acidic conditions

$$KAlSi_3O_8 + 4H_2O + 4H^+ \Leftrightarrow K^+ + Al^{3+} + 3Si(OH)_4$$

To continue weathering:

$$Al^{3+} + 3Si(OH)_4 + \tfrac{1}{2} H_2O \Leftrightarrow 3H^+ + \tfrac{1}{2} Al_2Si_2O_5(OH)_4$$

Accordingly, kaolinite can be formed as the result of combining soluble silica with soluble aluminum ion. Likewise, Alkali ions and silica will be released and reacted with other minerals or lost with water flow.

Progressive weathering of volcanic rocks made decomposition of all minerals possible except quartz. The presence of some impurities such as titania and iron oxide had negative effects on quality of kaolin. Titanium took place in small amounts, mainly in form of anatase from which dispersed form was difficult to determine by XRD (P. Fisher 1984). Correspondingly, small amounts

of iron went in kaolinite structure and replaced aluminum in octahedral layer (H.H. Murray and Keller 1993).

Chemical analysis

Atomic absorption spectroscopy (AAS) analysis was performed to determine the concentration of iron ions existing in aqueous solution of samples. The results of AAS analysis indicated the reduction of iron content by micro-organism. The AAS results of sample are shown in Table 3. This result demonstrated that soil micro-organism can reduce the amount of iron content to a third after 7 days. Though significant reductions have not been made after 14 days. Statistical analysis showed that differences between all groups were significant ($P<0.05$).

Table 3. *AAS analysis to determining the iron content of samples after bioleaching.*

Time (Days)	Iron content (ppm)
0	156.1±9.0
7	56.8±5.0
14	50.3±4.0

Microscopic studies

Scanning Electron Microscopic (SEM) analysis of the sample after bioleaching was completed in order to get an atomic level chemical composition of impurity minerals (Figure 3). The picture displays near usual kaolinite platelets. The EDS analysis indicated the presence of iron in two samples. Moreover, EDS result revealed that bioleaching had not made an important change in chemical composition of the samples (Table 4). But, there is a significant decrease in amount of Fe impurities (Fe Mass %), from 4.3 % to 2.5 % after bioleaching process.

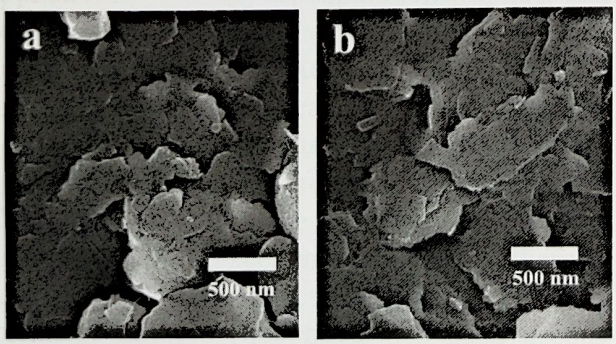

Fig. 3. *SEM micrographs of kaolin sample before and after microbial bioleaching (a) untreated kaolin, and (b) the bioleached kaolin.*

Table 4. *EDS analysis of Abadeh kaolin before and after microbial bioleaching.*

	Untreated kaolin (Mass%)	Treated kaolin (Mass%)
O	49.2	50.7
Al	16.8	16.6
Si	26.1	26.9
Fe	4.3	2.5
K	2.3	2.1
Na	1.3	1.2

Conclusions

The Abadeh kaolin sample which was taken for this study has different types of mineral species impurities. The major iron mineral species impurity is hematite along with pyrite as minor secondary mineral.

The results of AAS analysis before bioleaching demonstrated a large amount of iron impurity in kaolin clays, however, quality level of clay was increased after one-week of microbial treatment. Nevertheless, the quality of Abadeh clay has not been improved significantly by extending time of bioleaching. Regarding the decrease of iron impurity, it can be a good candidate to be used in ceramic and porcelain industries.

References

Adamis, Z., and Williams, R.B. 2005. *Bentonite, Kaolin, and Selected Clay Minerals (Environmental Health Criteria 231)*. WHO, Geneva.

Adefila, S S. 2012. Comparative Study of Chemical And Biological Methods of Beneficiation of Kankara Kaolin. **1**(8) : 13–18.

Cooper, D. Craig et al. 2005. Effects of Sediment Iron Mineral Composition on Microbially Mediated Changes in Divalent Metal Speciation: Importance of Ferrihydrite. *Geochimica et Cosmochimica Acta* **69** (7): 1739–54.

Ghorbani, Mansour. 2013. Metallogeny and Distribution of Minerals. In *The Economic Geology of Iran*, Springer Netherlands, 87–197.

Gonzalez, J. and Delcruiz, M. 2006. Bleaching of Kaolins and Clays by Chlorination of Iron and Titanium. *Applied Clay Science* **33**(3–4): 219–29.

Murray, H.H. and Keller, W.D. 1993. Kaolins, Kaolins and Kaolins. In: Kaolin Genesis and Utilization. *Clay Min. Soc., Spec. Pub* **1**: 1–24.

He, Qiu-xiang, Xiao-chen Huang, and Zu-Liang Chen. 2011. Influence of Organic Acids, Complexing Agents and Heavy Metals on the Bioleaching of Iron from Kaolin Using Fe(III)-Reducing Bacteria. *Applied Clay Science* **51**(4): 478–83.

Javaherdashti, Reza. 2008. Engineering Materials and Processes *Microbiologically Influenced Corrosion*. London: Springer London.

Mockovèiaková, A., Štyriaková Iveta, Škvarla Jiøí, and Kozáková Ivana. 2008. Characterization of Changes of Low and High Defect Kaolinite after Bioleaching. *Applied Clay Science* **39**(3–4): 202–7.

P. Fisher. 1984. Some Comments on the Color of Fired Clays. *Ziegel Industrie International* **37**: 475–83.

Shelobolina, Evgenya S., Sam M. Pickering, and Derek R. Lovley. 2005. Fe-Cycle Bacteria from Industrial Clays Mined in Georgia, USA. *Clays and Clay Minerals* **53**(6): 580–86.

Stucki, J.W., B.A. Goodman, and U. Schwertmann. 1988. Iron in Soils and Clay Minerals *Iron in Soils and Clay Minerals*.

Williamson, Adam J et al. 2013. Microbial Reduction of Fe(III) under Alkaline Conditions Relevant to Geological Disposal. *Applied and Environmental Microbiology* **79**(11): 3320–26.

Zegeye, Asfaw et al. 2013. Applied Clay Science Re Fi Nement of Industrial Kaolin by Microbial Removal of Iron-Bearing Impurities. *Applied Clay Science* **86**: 47–53.

(Received March 2017; Accepted May 2017)

Clay Research, Vol. 35, No. 2, pp. 61-70 (2016)

Functionalization and Formation of Drinking Water Filter Rod from Lignite with Zeolite, Bentonite, and Local Clay

SUMRIT MOPOUNG*, NIMIT SRIPRANG, JUTATIP NAMAHOOT, NANTAKA UMFANG, LALITA CHUAYUDOM, WEERADA RATTANPRASIT, SIRIWAN DI-INKAEW, KHATRIYA JANNACHAI, DUSADEEPORN POLKANYIM AND ROSJARAS BUNPUM

Department of Chemistry, Faculty of Science, Naresuan University, Phitsanulok, Thailand

Abstract–*A drinking water filter rod was functionalized and formed from a starting mixture of lignite, zeolite, bentonite, and clay. The formation of the filter was studied focusing on the effects of zeolite dosageand sintering temperature in a reducing atmosphere. Borax was also added to the starting mixtures for melting point reduction.The sintered filterswere characterized by XRD, FTIR, and SEM-EDS.The percent drying shrinkage, percent firing shrinkage, percenttotal shrinkage,percentmass yield, percentfixed carbon, and hardnessof filters weremeasured. The results showed that the firing shrinkage, the total shrinkage and hardness increased with increasing sintering temperature.The hardness of sintered filters ishigher thanthe limitof theThai Industrial Standards Institute.On the other hand, mass yield and fixed carbon decreased with increasing sintering temperature. The starting materials mixture of 45wt% lignite, 30wt% zeolite, 10wt% bentonite, 10wt% local clay, and 5wt% boraxwas used with sintering temperatures ranging from 400 °Cto 600°C. The functional surface groups of the sintered filter exhibited a high content of aluminosilicates and carbon, whichwere derived from all starting materials. The macropores of sintered filterhad dimensions of the channels between particles in the range of 0.2-2 μm.*

Key words : Drinkin gwater filter, functionalization, , zeolite, lignite sintering

Introduction

The capability to functionalize the interior channels and/or internal surface areas of porous inorganic solids with specific organic or inorganic moieties has dramatically expanded the potential applications in catalysis, separations, optical and optoel ectronic devices, drug delivery, sensors, and energy conversion (Athens *et al.*, 2009). Clay materials or aluminosilicates have been used as adsorbents, water softeners, catalysts, and mechanical and thermal reinforcement materials. They are used for these purposes due to their high surface area, excellent thermal/hydrothermal stability, high shape selectivity, and superior ion-exchange ability. They have also been usedas polymer fillers, which allowed to expand their application range to innovative areas such as medical and biological fields as well as sensors, filtration membranes, energy storage materials, and novel catalysts (Lopes *et al*, 2014). These materials possess a layered structure and are considered to act as host materials. The adsorption capabilities of these materials result from the net negative charge on thestructure of the minerals, which give clay the ability to adsorb positively charged species. Their adsorption properties are also related to their high surface-area and high porosity. There has been an increasing interest in utilizing clayminerals such as bentonite, kaolinite, and diatomite fortheir capacity to adsorb both inorganic and organic molecules (Ahmaruzzaman, *et al.*, 2008). In addition, the plastic property of clay is appropriate

***Corresponding Author Email :** sumritm@nu.ac.th

for processing through extrusion. Furthermore, after appropriate subsequent drying and heating treatments, these clay based materials become rigid solids with good physico-chemical properties (Gatica and Vidal, 2010). The natural zeolite has highcation-exchange capacityand exhibitshighadsorption capacity for methylene blue, rhodamine B (Wang and Zhu, 2006), and heavy metals (Shukla *et al*, 2009). However, it has a negligible adsorption capacity for organic contaminants from aqueous solution (Shukla *et al.*, 2009). Zeolites are hydrated aluminium-silicate mineralsin which the aluminium and silicon polyhedra are linked by thesharing of oxygen atoms (Vohla *et al*, 2011). They are highly porous aluminosilicates with different cavity structures. Their structures consist of a three dimensional framework,having a negatively charged lattice. The negative charge is balanced bycations which are exchangeable with certain cations in solutions (Ahmaruzzaman, 2008). Bentonite is another natural clay, which contains mainly the smectite and kaolinite mineral phases). These natural inorganic materials have potential for surface functionalization. For example, hybrid inorganic/organic adsorbents have been synthesized using mixtures of diatomite and carbon charcoalas precursors, which are used for the removal of p-cresol from aqueous solution (Hadjar *et al*, 2011). Montmorillonite clay has been used to prepare carbon/clay nanocomposites andcomposites by calcination in a reducing atmosphere. The adsorbent, which contains 45.94% zeolite, 15.31% limestone, 4.38% activated carbon, and rice husk carbon respectively, and 30% ofordinary Portland cement (as a binder), has been used for adsorption of chemical oxygen demand and ammoniacal nitrogen causing contaminants in landfill leachate treatment. A combination of activated carbon and zeolite, as a natural ion exchanger, in composite media provides both hydrophobic and hydrophilic surfaces for the removal organic and inorganic (especially ammonia) contaminants (Halim *et al*, 2010). In this composite, the carbon is essential to preserve the mesoporous structure of the source. Furthermore, the addition of aluminum on mesoporous silica is critical for the stability of the zeolitic building units on the surface of mesopores (Ogura *et al*, 2007).The granular X-type zeolite/activated carbon composites have been prepared from elutrilithe by adding pitch powder and solid SiO_2. The composites had a hierarchical pore structure andahigh content of carbon in the composites (Li *et al.*, 2014). The adsorption capacity of carbon-zeolite composites depends on carbon content. For example,the adsorption of phenol on carbon and natural zeolite composite is increased with increasing carbon content of the composite (Shukla *et al.*, 2009). The composite prepared by liquid phase impregnation of zeolite templates using lignin solutions as carbon precursor have high microporosity and mesoporosity. The templated carbon present surface chemistry with a relatively high amount of nitrogen and oxygen stable surface groups, such as pyrrolic, pyridinic, hydroxyl and carbonyl, which were formed by transfer of ammonia and oxygen from the surface of the zeolite template to the carbon materials during the synthesis (Valero-Romero *et al.*, 2014). Composite material consisting of activated carbon and zeolites has successfully been prepared using coal fly ash, which contains SiO_2, Al_2O_3, and unburned carbon. It was activated by NaOH fusion treatment at 750 °C in a N_2 atmosphere for conversion into zeolites Na–X and/or Na–A with good crystallinity by hydrothermal treatment (Miyake *et al*, 2008). Silica/activated carbon (2:3) composite with high efficiency in the removal of nickel ions has also been prepared (Karnib *et al*, 2014). These composites were used for many purposes. For example a composite adsorbent synthesized from activated carbon, silica-gel, and $CaCl_2$ has been used for adsorption cooling and dehumidification systems (Tso and Chao, 2012). A composite prepared from melamine-modified phenol–formaldehyde resinsvia steam activation at different activation temperatures (700–950 °C) was used for CO_2 capture at atmospheric pressure

(Tseng *et al.*, 2015). Solid sorbents derived from mixtures of montmorillonite, activated carbon, and cement have also been used for sorption of phenol and 4-nitrophenol (Houari *et al.*, 2014).

The aim of this research was to study the effects of zeolite dosage and sintering temperatures on the formation and functionalization of water filters using the addition of bentonite and local clay as binder. The composition of the filter and presence of functional groups after sintering was investigated by Fourier transform infrared spectrometry, X-ray diffraction, and scanning electron microscopy equipped with energy dispersive spectrometer.

Materials and Methods

Preparation of Materials

Zeolite (commercial grade), bentonite (commercial grade), local clay (obtained from Tambol Tapoh, Muang District, Phitsanulok Province, Thailand), and lignite (obtained from the Mae Moh Basin, Lampang Province, Thailand) were ground and sieved (Laboratory test sieve, Retsch, Germany) to 200 mesh. These materials were mixed to prepare mixtures containing zeolite (5, 10, or 30wt%), bentonite (10wt%), clay (10wt%), and charcoal (60, 90,or 95wt%). The mixtures of starting materials were wetted with water (20% by volume) and borax (5wt%, commercial grade) was added.The thermal behavior of the starting mixtures was investigated by differential scanning calorimetry (DSC-1, Mettler). The wetted mixtures were pressed into a PVC pipe (f = 12.7 mm, long = 50 mm). The percent of drying shrinkage, percent of firing shrinkage of the samples were measured by the methods of de Sa, *et al*,(2008) and Rasmussen *et al*, (1997), respectively. The percent mass yields of sintered filters were also measured. The wetted samples were dried in an oven for 24 h. The dried samples were then placed intoa ceramic box and covered with foil, quartz powder, and closed by a lid. The samples were then sintered in an electric furnace (Fisher Scientific IsotempÒ Muffle furnace) under are ducing atmosphere at temperatures of 400ºC, 500 ºC,600 ºC, or 700ºC with 1 h soaking time. Triplicate samples were used for all experiments. The sintered samples were characterized by X-ray powder diffractometer (XRD, PW 3040/60, X' Pert Pro MPD) with a Cu tube anode, a Fourier transform infrared spectrometer (Spectrum GX, Perkin Elmer), and scanning electron microscope equipped with energy dispersive spectrometer (SEM-EDS, LEO 1455 VP).

Results and Discussion

Differential scanning colorimeter (DSC) study shows

The endothermic peak of a representative DSC curve obtained from pyrolysis of mixture of starting materials in pure N_2 (Figure 1) shows the peak at149.11 ºCattributable to endothermic evaporation of volatile moisture (Slaty *et al*, 2013). In general, peaks in the rangeof 100-150 ºC can be attributed to low-temperature physical desorption of water and gases (Boycheva *et al*, 2013). The minor peaks at 480 and 550 ºC are attributed to dehydroxylation, which is the removal of hydroxyl groups from Al-OH bonds (Slaty*et al*, 2013). These results are in line with the FTIR data (Figure 3d), in which the OH group of sintered filter materials disappeared. It was observed that the degradation of the mixture of starting materials is low, which results in no firing shrinkage of sintered filters obtained at 400 ºC. Mixing with zeolite only or a mixture of zeolite, bentonite, and clay could improve the formation of the mixture of the starting materials by wet method considerably affects compressive strength. Bentonite is an inorganic binder capable of improving strength of resulting composite materials (Salem and Sene, 2011). However, these mixtures are forming after sintering at 400-700 ºC. The carbon content of sintered samples obtained at 700 ºC is also reduced. because of

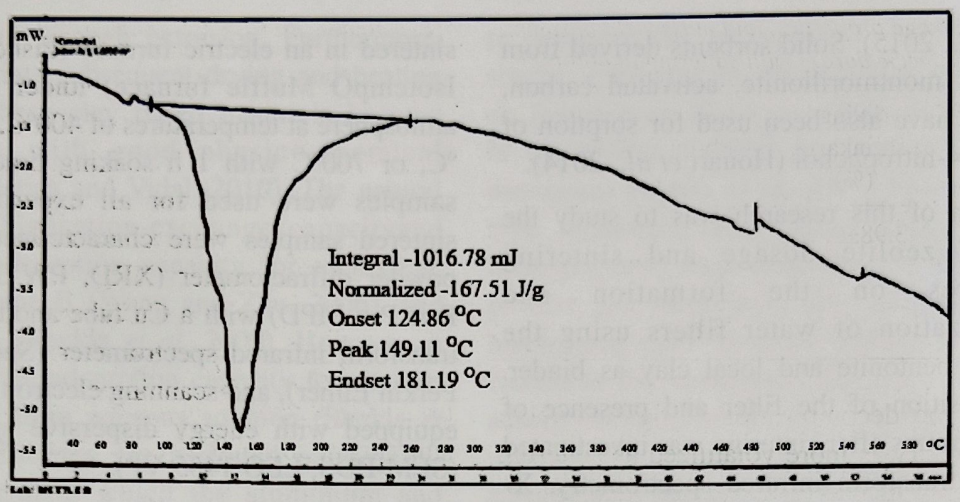

Fig. 1. *DSC curve of the mixture of starting materials (45wt% lignite, 30wt% zeolite, 10wt% bentonite, 10wt% local clay, and 5wt% borax).*

decomposition of carbon due to the catalytic effects of zeolite surface and deeper volatilization ofthe carbon at high temperatures (Valero-Romero *et al*, 2014). On the other hand, the mixtures containing 5wt% borax additive could be formablefrom temperature above 400 °C, as shown in Figure 2. Since borax is a fluxing reagent (Jie *et al*, 2008), it can be reduced at the sintering temperatures (Salem and Aghahosseini, 2012) of these mixtures. Salem and Sene (2011) have reported that mixtures with high content of zeolite, bentonite, and kaolin could be forming at ≥ 600 °C. However, the mixtures in this study were mixed with lignite, which is quite volatile at high temperatures. Some carbon content of lignite was volatized after sintering. This effect caused the reduction of strength of sintered samples with formability.

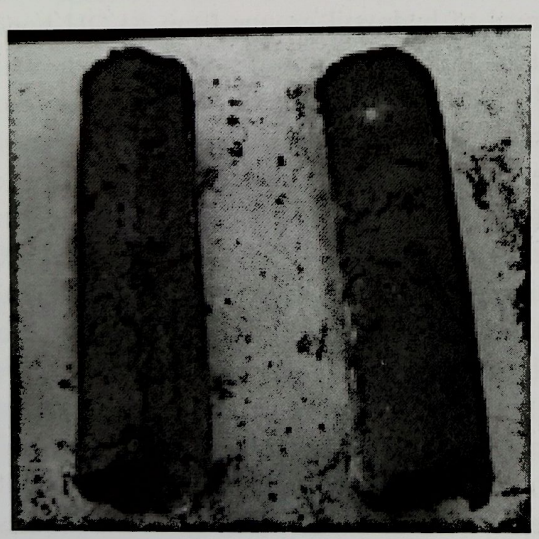

Fig. 2. *Filter sample developed after sintering at 400 °C. (materials (45wt% lignite, 30wt% zeolite, 10wt% bentonite, 10wt% local clay, and 5wt% borax)*

The drying shrinkage, firing shrinkage and total shrinkage properties of material

The percent of drying shrinkage, firing shrinkage, and total shrinkage were determined only for filters prepared from 45wt% lignite, 30wt% zeolite, 10wt% bentonite, 10wt% local clay, and 5wt% borax at sintering temperature of 400-600 °C, as shown in Table 1. It was shown that the firing shrinkage increased with the increase in sintering temperature. Consequently the total shrinkage increased with increasing sintering temperature as well. It was observed that the sintered filter prepared at 400 °C has no firing shrinkage. This may be due to very low degradation of the aluminosilicate compounds at this temperature (Liu *et al.*, 2009). The mass yield of the filters decreased with increasing sintering temperature. The mass loss involved dehydroxylation of kaolinite, with the removal of hydroxyl groups from Al-OH bonds (Slaty *et*

Table 1. *Shrinkage properties, and mass yield of sample (45 wt% lignite, 30 wt% zeolite, 10 wt% bentonite, 10wt% local clay, and 5wt% borax) with sintering at 400-600 °C*

Temperature °C	drying shrinkage (%)	firing shrinkage (%)	Total shrinkage (%)	Mass yield (wt%)	Fixed carbon (wt%)	Hardness (kg/cm^2)
110	3.98±0.23	-	-	-	21.26	53.59
400	-	0.00±0.00	3.98±0.12	89.59±0.24	28.39	7.84
500	-	4.01±0.17	7.99±0.20	87.67±0.37	22.32	10.10
600	-	4.35±0.14	8.33±0.19	76.52±0.32	11.66	15.05

al., 2013), and decomposition of lignite, where carbon content was more volatilized as sintering temperature is increased (Valero-Romero *et al*, 2014). It was observed that the mass yields of sintered filters are relatively high. This is because zeolite, bentonite, and clay are inorganic materials which are thermally stable (Athens *et al*, 2009). Thus the amount of fixed carbon in sintered filters decreased with increasing sintering temperature, resulting in concomitantdecrease of mass yield. It was shown that the mass yield of sintered filters depends on decomposition of carbon content in the mixtures. In addition, it was observed that the fixed carbon content of mixture after drying at 110 °C is relatively low when compared to the sintered filters. This is because of the high content of volatile matter in lignite (69.02 wt%, Mopoung *et al.*, (2008), which results inlower carbon content.

The hardness of sintered filters increased with increasing sintering temperature. This may be attributed to the decreasing porosity of sintered filters as sintering temperature increases, which is the result of dehydroxylation and decomposition during sintering (Hoepfner and Case, 2003). This result is directly related withthe reduction of carbon content of sintered filter as function of increasing sintering temperature. It could reflect that the sintered filter has higher interfacial strength with good interconnectedness as a result of higher sintering temperature (Guiderdoni *et al.*, 2011). The hardness of all sintered filters is higher thanthe limitset by the Thai Industrial Standards Institute (700±10 kPa or 7.1380 kg/cm^2). Sintered filters obtained with sintering at 500-600 °C have hardness comparable to strong pelletized grey alder wood base activated carbon sintered at 600 °C (Rizhikovs *et al.*, 2012). However, the hardness of all sintered filters is lower than the hardness of starting lignite. This is due to the release of volatile material from all starting materials at high temperature (Msagati *et al.*, 2014). Thus, all of the sintered filters are softened.

Due to the results discussed above, the filter obtained by sintering at 400 °C was used for further characterization as it had lowest shrinkages and a higher standard hardness.

X-Ray diffraction analysis

Figure 3a shows the X-ray diffractogram of lignite. The background intensity of XRD,seems to be high and exhibits signals of highly disordered materials in the form of amorphous carbon (Msagati *et al*, 2014) in both lignite and sintered filter. The main mineralogical component of lignite are kaolinite ($Al_2Si_2O_5(OH)_4$), montmorillonite ($Na_{0.33}(Al_{1.67}Mg_{0.33})\ Si_4O_{10}(OH)_2$), quartz ($SiO_2$), calcite ($CaCO_3$), muscovite ($KAl_2(AlSi_3O_{10})\ (OH)_2$)/illite ($K_{1.5}Al_4(Si_{6.5}Al_{1.5})\ O_{20}(OH)_4$), and boehmite (AlO(OH)), which are common in lignite (Zhao *et al.*, 2012). Peaks of crystalline order of some graphite in lignite have been detected at 26.5°,44.5° and 53.5° (Hongqiang *et al*, 2013). The peaks in the diffractogram attributed to kaolinite are at 12.5°,20°, 23.1°, 25.5°, 28.1°, 39°, 55.5°, and 56.9° (Slaty *et al*, 2013). Peaks at 27.9° and 42.8° correspond to

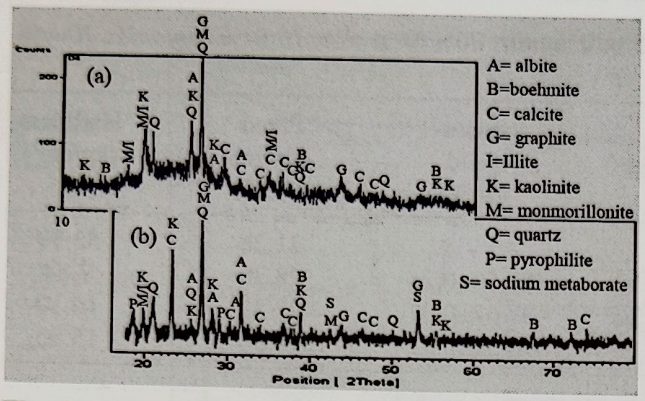

Fig. 3. *X-ray diffraction patterns of (a) lignite and (b) filter obtained with sintering at 400 °C.*

montmorillonite. Furthermore, peaks corresponding toquartz, can be found at 21°, 26.8°, 36.5°, 39.5°, 50.1°, 52.3°, 55°, 60°, and 68.1° (Slaty *et al.*, 2013). The peaks of calcite appear at 29.5°, 31.8°, 33.9°, 35°, 37°, 38°, 46.2°, 47.9°, and 74°. The peaks at 18°, 20° and 35° corresponded to muscovite/illite (Slaty *et al*, 2013). Peaks of boehmite were found at 15°, 39°, 55.5°, 67.2°, and 72.1° (Zhao *et al.*, 2012). Finally, albite is also common component in lignite found at very low concentrations. The peaks of albeit occur at 25.5°, 28.1°, 31°, and 31.9° (Zhao *et al.*, 2012).

After modification with zeolite, bentonite, and clay the sintered filter contained kaolinite, montmorillonite, quartz, calcite, muscovite/illite and boehmite as its components (Figure 3b). Furthermore, pyrophilite is also found in the sintered filter with peaks at 19.2°, 29°, and 35°. These minerals are found in zeolite, bentonite, and clay (Salem and Sene, 2011) as well as in lignite (Zhao *et al*, 2012). Additional peaks attributed to sodium metaborate ($NaBO_2$) were found 53.46° and 42.30° in the filter (Park *et al*, 2007). Sodium metaborate was produced from borax ($Na_2B_4O_7$) by chemical reaction with metal oxide (Shen *et al.*, 2012).

FTIR analysis

It can be seen from Figure 4 that zeolite and bentonite have almost identical vibrational bands. It was shown that the surface functional groups of both are similar since both materials are aluminosilicates (Lee *et al*, 2015; Vohla *et al*, 2011). The surface functional groups of the filter (Figure 4d) seem tobe the sum of the functional groups of all raw materials (Figure 4a-c). The peak at about 3650 cm^{-1}, which originated from zeolite (Figure 4a) and bentonite (Figure 4b), can be attributed to the AlO-H groups and bridging acidic hydroxyls Si-O(H)-Al. The weak peak at 3750 cm^{-1}, which originated from zeolite (Figure 4a), can be attributed to SiO-H groups. The broad band found at 3200-3400 cm^{-1}, which belongs to lignite (Figure 4c), and the peak at 1633 cm^{-1}, which belongs to zeolite (Figure 4a) and bentonite (Figure 4b), disappeared after sintering at 400 °C. These features are associated with Si-OH stretching and O-H stretching vibrations of adsorbed water molecules (San Cristóbal *et al.*, 2010). It was shown that the adsorbed water molecules were removed after sintering at 400 °C. The very weak peaks found at about 2850 cm^{-1} and 2950 cm^{-1} of lignite, due to C-H_2 stretching (Liu *et al.*, 2015), disappeared after sintering. The vibration bands appearing around 1010 cm^{-1} and between 800 and 400 cm^{-1} are attributed to the characteristic behavior of aluminosilicate containing materials. The weak peak at around 800 cm^{-1} can be associated with Al–O or Si–O symmetric stretching vibrations. Furthermore, the strong band at about 1010 cm^{-1},

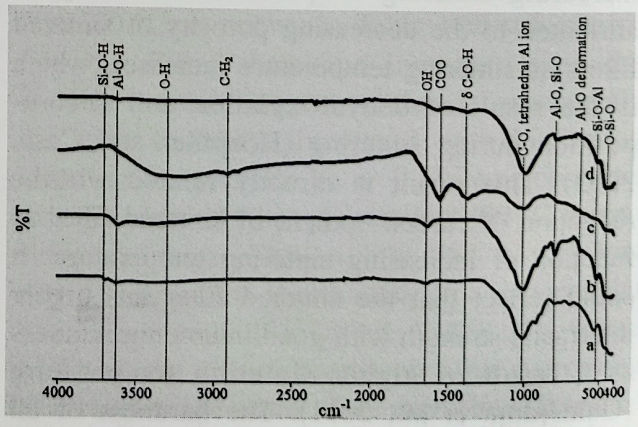

Fig. 4. *FTIR spectra of (a) zeolite (b) bentonite (c) lignite and (d) filter obtained with sintering at 400 °C.*

found in all of the materials, was attributed totetrahedral Al ions (San Cristóbal *et al*, 2010) or CO (Tseng *et al.*, 2015). This peak also remained in the filter. The two peaks at about 1554 cm^{-1} and 1350 cm^{-1} of lignite were attributed to carboxylates and/or metal-bonded carboxylates (Gezici *et al*, 2012). These peaks remained in filter. However, the peak at 1350 cm^{-1} found in the filter may be also due to B–O originating from $Na_2B_4O_7$ (Park *et al*, 2007). The intensity of these peakis weakening after sintering. It was shown that some carboxylate groups were removed during sintering. The weak peak at 630 cm^{-1} for bentonite (Figure 4b) was assigned to Al–O deformation (Musyoka *et al*, 2014). This peak remained in the filter after sintering. The vibration bands of Si–O–Al (540 cm^{-1}) in tetrahedral and octahedral sheets of kaolinite, and O–Si–O(480 cm^{-1}) (San Cristóbal *et al*, 2010) from zeolite and bentonite were found in the sintered filter. These functional groups are expected to contribute to ion-exchange processes as well as adsorption process for the removal of heavy metal cations (Weiwei *et al*, 2013).

SEM analysis

Figure 5 shows the SEM micrographs of lignite (Figure 5a) and sintered filter obtained with sintering at 400 °C (Figure 5b). Lignite has open porous, rough surface and quite dense texture supporting its high hardness (Table 1). The sintered filter has channels as well as arough surface. The channel size between particles is in the range of 0.2 to 2 μm (Figure 5b). The channels and surface of lignite particles appear dispersed in between the clay or alumino-silicate mineral with a heterogeneous distribution. It was observed that the sintered filter has higher porosity and lower density than lignite. This was attributed to the reduction of elemental carbon, volatile matter content, and dehydroxylation of mixture of the starting materials during sintering (Hoepfner & Case, 2003). Another reason is the high porosity of zeolite and bentonite. The macro-pores on the surface of sintered filter have been observed. These can facilitate the flow of water (Thapa *et al.*, 2009). EDS results revealed that the composition of filter obtained with sintering at 400 °C is 29.07 wt% C, 22.90 wt% O, 18.15 wt% Al, 22.42 wt% Si, 2.12 wt% Na, 0.63 wt% Mg, 1.45 wt% K 0.57 wt% Ca, 1.59 wt% Fe, and 1.07wt% B. These results showed a high concentration of carbon in the sintered filter, which is comparable to the carbon content inzeolite/activated carbon composites produced with calcination at 450 °C and activation at 850 °C (Li *et al*, 2014). The sintered filter is also abundantin O, Al, and Si, which correlates well with the XRD results. It was showed that the all of the elements are present in the form of oxides (Tozsin, 2014).

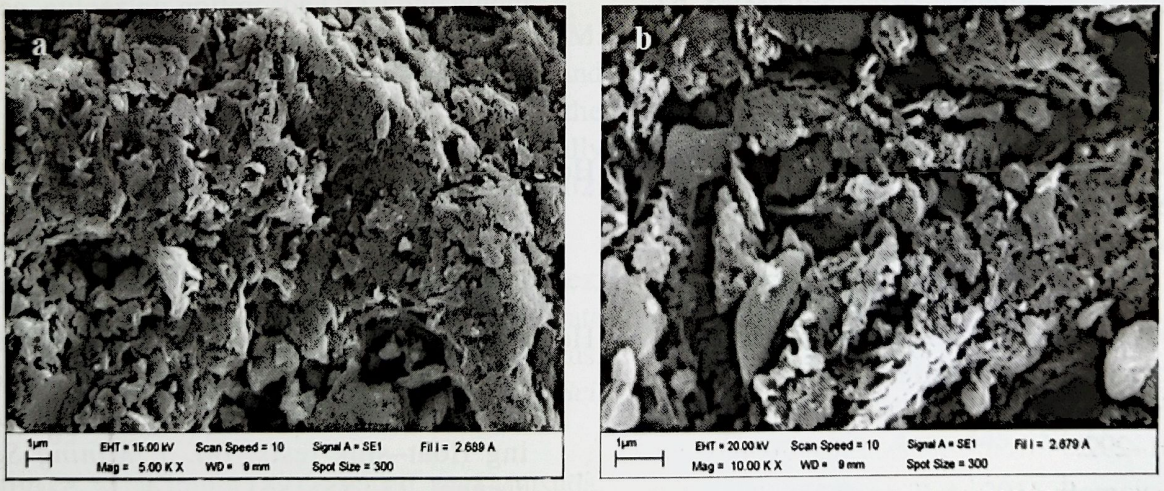

Fig. 5. *SEM morphology of (a) lignite (b) filter obtained with sintering at 400 °C.*

Conclusions

Sintered filters wereprepared from mixtures of lignite, zeolite, bentonite, and clay. These filters arefunctionalizated and have a high content of aluminosilicatesand carbon. The firing shrinkage, the total shrinkage, and hardness of sintered filters increased with increasing sintering temperature from 400 °C to 600 °C. The hardness of sintered filters is more than700±10 kPa or 7.1380 kg/cm^2. The porosity of the sintered filter is higher than that of the starting material lignite.The sintered filter made frommixture containing 45wt% lignite, 30wt% zeolite, 10wt% bentonite, 10wt% local clay, and 5wt% borax and sintered 400 °C has potential to be used for heavy metal removal from aqueous solutions via cation exchange and adsorption processes.

Acknowledgement

The authors would like to thank the Chemistry Department, Faculty of Science, Naresuan University for the support of this project.

References

Ahmaruzzaman, M. 2008. Adsorption of phenolic compounds on low-cost adsorbents: A review. *Adv. Colloid Interfac. Sci.*143:48–67.

Anadão, P., Pajolli, I.L.R., Hildebrando, E.A. and Wiebeck, H. 2014. Preparation and characterization of carbon/montmorillonite composites and nanocomposites from waste bleaching sodium montmorillonite clay. *Adv. Powder Technol.* **25** : 926–932.

Athens, G.L., Shayib, R.M. and Chmelka, B.F. 2009. Functionalization of mesostructured inorganic–organic and porous inorganic materials. *Curr. Opin. ColloidInterfac. Sci.* **14** : 281–292.

Boycheva, S., Zgureva, D. and Vassilev, V. 2013. Kinetic and thermodynamic studies on the thermal behaviour of fly ash from lignite coals. *Fuel* **108**: 639–646.

de Sa, C., Benboudjema, F., Thiery, M. and Sicard, J. 2008. Analysis of microcracking induced by differential drying shrinkage.*Cement Concrete Comp.* **30** : 947–956.

Gatica, J.M. and Vidal, H. 2010. Non-cordierite clay-based structured materials for environmental applications. *J. Hazard. Mater.* **181**: 9–18.

Gezici, O., Demir, I., Demircan, A., Ünlü, N. and Karaarslan, M. 2012. Subtractive-FTIR spectroscopy to characterize organic matter in lignite samples from different depths. *Spectrochim. Acta A* **96** : 63–69.

Guiderdoni, Ch., Estournès, C., Peigney, A., Weibel, A., Turq, V. and Laurent, Ch. 2011. The preparation of double-walled carbon nanotube/Cucomposites by spark plasma sintering, and their hardnessand friction properties. *Carbon* **49**: 4535–4543.

Hadjar, H., Hamdi, B. and Ania, C.O. 2011. Adsorption of p-cresol on novel diatomite/carbon composites. *J. Hazard. Mater.* **188** : 304–310.

Halim, A.A., Aziz, H.A., Johari, M.A.M. and Ariffin, K.S. 2010. Comparison study of ammonia and COD adsorption on zeolite, activated carbon and composite materials in landfill leachate treatment. *Desalination* **262**: 31–35.

Hoepfner, T.P. and Case, E.D. 2003. The influence of the microstructure on the hardness of sintered hydroxyapatite. *Ceram. Int.* 29 : 699–706.

Hongqiang, L., Qiming, F., Leming, O., Sisi, L., Mengmeng, C. and Xiaoqing, W. 2013. Study on washability of microcrystal graphite using float–sink tests. *Int. J. Mining Sci. Technol.* **23** : 855–861.

Houari, M., Hamdi, B., Bouras, O., Bollinger, J.-C. and Baudu, M. 2014. Static sorption of phenol and 4-nitrophenol onto composite geomaterials based on montmorillonite, activated carbon and cement.*Chem. Eng. J.* **255**: 506–512.

Jie, L., Mei-fang, D., Bo, Y. and Zhong-xiao, Z. 2008. Quantum and experimental study on coal ash fusion with borax fluxing agent. *J. Fuel Chem. Technol.* **36** : 519–523.

Karnib, M., Kabbani, A., Holail, H. and Olama, Z. 2014. Heavy metals removal using activated carbon, silica and silica activated carbon composite. *Energ. Procedia* **50** : 113–120.

Lee, S.M., Lalhmunsiama, Thanhmingliana and Tiwari, D. 2015. Porous hybrid materials in the remediation of water contaminated with As(III) and As(V). *Chem. Eng. J.* **270** : 496–507.

Li, Z., Cui, X., Ma, J., Chen, W., Gao, W. and Li, R. 2014. Preparation of granular X-type zeolite/activated carbon composite from elutrilithe by adding pitch and solid SiO_2. *Mater. Chem. Phys.* **147** : 1003–1008.

Liu, X., Gao, F. and Tian, C. 2009. Sandwich layer composite prepared by a novel zero-shrinkage-difference technology. *J. Alloy Compd.* **486** : 743–746.

Liu, Z. S., Peng, Y. H., Huang, C. Y. and Hung, M. J. 2015. Application of thermogravimetry and differential scanning calorimetry for the evaluation of CO_2 adsorption on chemically modified adsorbents. *Thermochim. Acta* **602**: 8–14.

Lopes, A.C., Martins, P. and Lanceros-Mendez, S. 2014. Aluminosilicate and aluminosilicate based polymer composites: Present status, applications and future trends. *Prog. Surf. Sci.* **89** : 239–277.

Miyake, M., Kimura, Y., Ohashi, T. and Matsuda, M. 2008. Preparation of activated carbon–zeolite composite materials from coal fly ash. *Micropor. Mesopor. Mat.* **112** : 170–177.

Mopoung, S., Anuwetch, L. and Inkum, S. 2008. Properties of activated carbon from lignite. *NU. J.* 16 : 127–130.

Msagati, T.A.M., Mamba, B.B., Sivasankar, V. and Omine, K. 2014. Surface restructuring of lignite by bio-char of Cuminumcyminum –Exploring the prospects in defluoridation followed by fuel applications.*Appl. Surf. Sci.* **301** : 235–243.

Musyoka, N.M., Missengue, R., Kusisakana, M. and Petrik, L.F. 2014.Conversion of South African clays into high quality zeolites. *Appl. Clay Sci.* **97–98** : 182–186.

Ogura, M., Zhang, Y., Elangovan, S.P. and Okubo, T. 2007. Formation of ZMM-n: The composite materials having both natures of zeolites and mesoporous silica materials. *Micropor. Mesopor. Mat.* **101** : 224–230.

Park, E.H., Jeong, S.U., Jung, U.H., Kim, S.H., Lee, J., Nam, S.W., Lim, T.H., Park, Y.J. and Yu, Y.H. 2007. Recycling of sodium metaborate to borax. *Int. J. Hydrogen Energ.* **32** : 2982–2987.

Rizhikovs, J., Zandersons, J., Spince, S., Dobele, G. and Jakab, E. 2012. Preparation of granular activated carbon from hydrothermally treated and pelletized deciduous wood. *J. Anal. Appl. Pyrol.* **93**: 68–76.

Rasmussen, S.T., Ngaji-Okumu, W., Boenke, K. and O'Brien, W.J. 1997. Optimum particle size distribution for reduced sintering shrinkage of a dental porcelain. *Dent. Mater.* **13**: 43-50.

Salem, A. and Aghahosseini, S. 2012. Determination of fluxing agents mixing ratio for enhancing thermal shockresistance of ceramic Raschig ring via a systematic approach. *Thermochim. Acta.* **545** : 57–66.

Salem, A. and Sene, R.A. 2011. Removal of lead

from solution by combination of natural zeolite–kaolin–bentonite as a new low-cost adsorbent. *Chem. Eng. J.* **174** : 619–628.

San Cristóbal, A.G., Castelló, R., Luengo, M.A.M. and Vizcayno, C. 2010. Zeolites prepared from calcined and mechanically modified kaolins: A comparative study. *Appl. Clay Sci.* **49** : 239–246.

Shen, M.J., Wang, X.J. and Zhang, M.F. 2012. High-compactness coating grown by plasma electrolytic oxidation on AZ31 magnesium alloy in the solution of silicate–borax. *Appl. Surf. Sci.* **259** : 362–366.

Shukla, P.R., Wang, S., Ang, H.M. and Tadé, M.O. 2009. Synthesis, characterisation, and adsorption evaluation of carbon-natural-zeolite composites. *Advanced Powder Technology,* **20**: 245–250.

Slaty, F., Khoury, H., Wastiels, J. and Rahier, H. 2013. Characterization of alkali activated kaolinitic clay. *Appl. Clay Sci.* **75–76** : 120–125.

Tozsin, G. 2014. Hazardous elements in soil and coal from the Oltu coal mine district, Turkey. *Int J. Coal Geol.* **131** : 1–6.

Tseng, R. L., Wu, F. C. and Juang, R. S. 2015. Adsorption of CO_2 at atmospheric pressure on activated carbons prepared from melamine-modified phenol–formaldehyde resins. *Sep. Purif. Technol.* **140** : 53–60.

Tso, C.Y. and Chao, C.Y.H. 2012. Activated carbon, silica-gel and calcium chloride composite adsorbents for energy efficient solar adsorption cooling and dehumidification systems. *Int. J. Refrig.***35**: 1626–1638.

Thapa, K.B., Qi, Y., Clayton, S.A. and Hoadley, A.F.A. 2009. Lignite aided dewatering of digested sewage sludge. *Water res.* **43** : 623–634.

Valero-Romero, M.J., Márquez-Franco, E.M., Bedia, J., Rodríguez-Mirasol, J. and Cordero, T. 2014. Hierarchical porous carbons by liquid phase impregnation of zeolitetemplates with lignin solution. *Micropor. Mesopor. Mat.***196** : 68–78.

Vohla, C., Koiv, M.,Bavor, H.J., Chazarenc, F. and Mander, U. 2011. Filter materials for phosphorus removal from wastewater in treatment wetlands—A review. *Ecol. Eng.* 37 : 70–89.

Wang, S. and Zhu, Z.H. 2006. Characterisation and environmental application of an Australian natural zeolite for basic dye removal from aqueous solution. *J. Hazard. Mater.* B **136** : 946–952.

Weiwei, B., Lu, L., Haifeng, Z., Shucai, G., Xuechun, X., Guijuan, J., Guimei, G. and Keyan, Z. 2013. Removal of Cu^{2+} from aqueous solutions using Na-A zeolite from oil shale ash. *Chinese J. Chem. Eng.* **21** : 974–982.

Zhao, Y., Zhang, J. and Zheng, C. 2012. Transformation of aluminum-rich minerals during combustion of a bauxite-bearing Chinese coal. *Int. J. Coal Geol.* **94** : 182–190.

(Received February, 2017; Accepted May, 2017)

Clay Research, Vol. 35, No. 2, pp. 71-83 (2016)

Creating the Optimal Product Formula for use by A Heavy Clay Block Manufacturer

ROGER MYLAN [a], CHRIS MAHARAJ [a] AND REAN MAHARAJ [b]*

[a] *Department of Mechanical and Manufacturing Engineering, The University of the West Indies, St. Augustine Campus, St. Augustine, Trinidad.*
[b] *Process Engineering, The University of Trinidad and Tobago, Point Lisas Campus, Brechin Castle, Trinidad.*

Abstract–*In order to address major quality defects such as cracking, excessive shrinkage and unsatisfactory product color in the final brick product being produced by a major clay block manufacturer in Trinidad, the non-optimization of block ingredients was investigated as the possible root cause for the defects. The effect of incremental deviations of the proportion of clay and sand to the original formulation on physical characteristics of compressive strength and modulus of rupture, and the aesthetic property of color was investigated. Scanning electron microscopy energy dispersive x-ray spectroscopy was conducted to measure the effectiveness of mixing in the preparation of the blends along with the elemental composition and distribution at the surface of the samples. The results indicated that at the statistical 95% confidence level, a 2.5% addition of clay to the original formulation resulted in a significant increase in compressive strength (89%) and modulus of rupture (58%). An improvement in the color aesthetic was also observed. The presence of homogenous elemental distributions indicated by SEM and elemental mapping studies indicated homogenous mixing. The presence of aluminum atoms (from the clay material in the form of kaolinite) suggests that the added clay (kaolinite) facilitates increased inter-particle bridging, increasing adhesion and cohesion characteristics thus, improving compressive strength and modulus of rupture as observed.*

Introduction

According to Guggenheim and Martin (1995), clay is a naturally occurring material whose primary composition is fine grained minerals, which is generally plastic at appropriate water contents and will harden when dried or fired. Although clay usually contains phyllosilicates, it may contain other materials that impart plasticity and harden when dried or fired. A brick or block can be composed of molded quantity of clay-bearing soil, containing sand and lime or cement, which is usually fire hardened or air dried and is the most common type used as they are the longest lasting and strongest building material. Its usage has been traced as early as 2900 BC in early Indus Valley cities (Possehl, 2002). A typical clay brick consist of silica (sand sized) 50% to 60%, alumina (clay size) – 20% to 30%, Lime – 2 to 5%, Iron oxide ≤ 7% and Magnesia – less than 1% (Punmia *et al.*, 2003).

Trinidad and Tobago, an oil and gas based industrialized economy, is one of the largest producers of clay blocks in the Caribbean region. The industrial production of bricks utilizes mainly the Grey Gumbo and Red Mottle clay types formulated with sand (predominantly silicon dioxide with a trace amount of aluminum oxide) and water in its manufacturing process (Ramdath, 2012). There exists other sources of clays of which the ceramic producing potential of several

***Corresponding Author Email :** rean.maharaj@utt.edu.tt (R. Maharaj)
Address : The University of Trinidad and Tobago, Point Lisas Campus, Brechin Castle, Trinidad., Trinidad Tel.: 00 1 868 6428888

has been investigated (Knight *et al.*, 1996; Knight 1996; Knight and Hosein, 1997)

The source of the clays used in the manufacture of ceramics together with the relative proportions of the ingredients used in the mixing formulations play a key role in the determination of the ultimate physical and performance properties of the ceramic end product as the inherent mineral and chemical composition influence their plasticity, drying, unfired and fired characteristics (Aras, 2004; Onal and Sarykaya, 2009). In almost every application involving clays, the clays and clay minerals are functional and are not just inert components in the system (Murray, 2000).

Early studies conducted by Davidson (1963) on Canadian manufactured clay-shale blocks showed that the compressive strength values of the final products varied when different raw materials were used. Ceramic formulation containing varied amounts of extruded kaolinite clay, silt and sand, produced samples that had unfired compressive strengths that varied between 1 and 4 MPa, with compressive strength decreasing as moisture content increased (Maskell *et al.,* 2013). A kaolinite clay based formulation extracted from a Trinidad mud volcano effluent containing additional quartz, mica and potash feldspar, had an unfired compressive strength of 1.9 MPa and mean linear shrinkage of 5.7 percent (Knight *et al.,* 1997) while a compressive strength of 2.5 MPa was obtained for a natural bentonite clay based block from Burgsvik, Sweden (Pusch, 2006). Research conducted on the firing characteristics of various Trinidad clays clearly demonstrated the relationship between composition of the clay (due to differences in source) and its fired properties. For example, it was found that when the clays were fired between 1000 and 1100 °C, the ceramic product made using Cocoloco and La Brea clays had higher strengths, toughness and lower porosities but significantly higher shrinkage compared to Valencia clay. The relatively higher shrinkage of the Cocoloco and La Brea clays had been associated with its relatively higher composition of soluble sulphates. The Valencia clay displayed a near white burning characteristic due to its relatively low iron content (Knight *et al.*, 1997).

In recent times, a principal producer of the brick manufacturing industry had been experiencing major quality constraints such as cracking, excessive shrinkage in the final brick product, as well as unsatisfactory product color. Such defects, if not mitigated, may damage the finances of the manufacturer. The raw material formula used by this producer is 52% clay, 18% silt and 30% sand. The addition of water is not measured, instead enough is added to allow for the workability of the material. Since the relationship between the composition and the primary physical, performance and rheological properties of clay based ceramic materials is well documented (Andreola *et al.,* 2004), one of the possible root causes for these defects had been associated with non-optimization of block ingredients.

The objectives of this study was to optimize the proportions of the clay and sand used by the manufacturer of the bricks by measuring the effect of incremental deviations of each ingredient to the original formulation on physical characteristics of compressive strength, modulus of rupture (flexural strength), and the aesthetic property of color.

Method

Specimen Preparation

Clay and sand were used as per specifications described. The materials were oven dried at a temperature of 60° C and the particle size range < 1 mm were collected for blending. Twenty five different blends containing various proportions of clay and sand were produced, which were then added to the base material formula.

The dried materials of each blend were thoroughly mixed, then combined enough water to allow for kneading. The materials were then hand kneaded and consolidated in a mixing bowl, to best simulate the mechanical processes utilized in the plant. The efficiency of mixing was investigated using Scanning Electron Microscopy by observing the distribution of these elements within the sample matrix.

The consolidated material was then transferred to the hand held extruder and compressed using the Hounsfield model H50K Universal Testing Machine to produce continuous lengths of 12 mm × 12 mm cross-section extruded material. These were cut into seven (7) 25 mm specimens for compressive strength testing and seven (7) 50 mm lengths for flexural strength testing. The labelled specimens were dried and fired using a Unifurnaces Ltd tunnel dryer kiln.The samples were analyses using a modified ASTM C67 – 11: Standard Test Methods for Sampling and Testing Brick and Structural Clay Tile (ASTM International 2011). The modification of the method was necessary as full sized block specimens of the various blends could not be obtained as this would have affected the existing plant operations.

Compressive Strength

The compressive strength tests were conducted using a Hounsfield model H50K Universal Testing Machine accordance to ASTM C67-11.

Flexural Strength

The flexural strength, termed the modulus of rupture (MOR), was found by the three (3) point bend method as described in accordance to ASTM C67-11.

Flexural Strength

The fired samples were analyses by a Konica Minolta CR-400 colorimeter with am illumination area of 8mm. Five samples per blend were tested and the averages were tabulated. The tests were carried using recommendations in AS 4459.16-2005 Methods of sampling and testing ceramic tiles - Determination of small color differences.

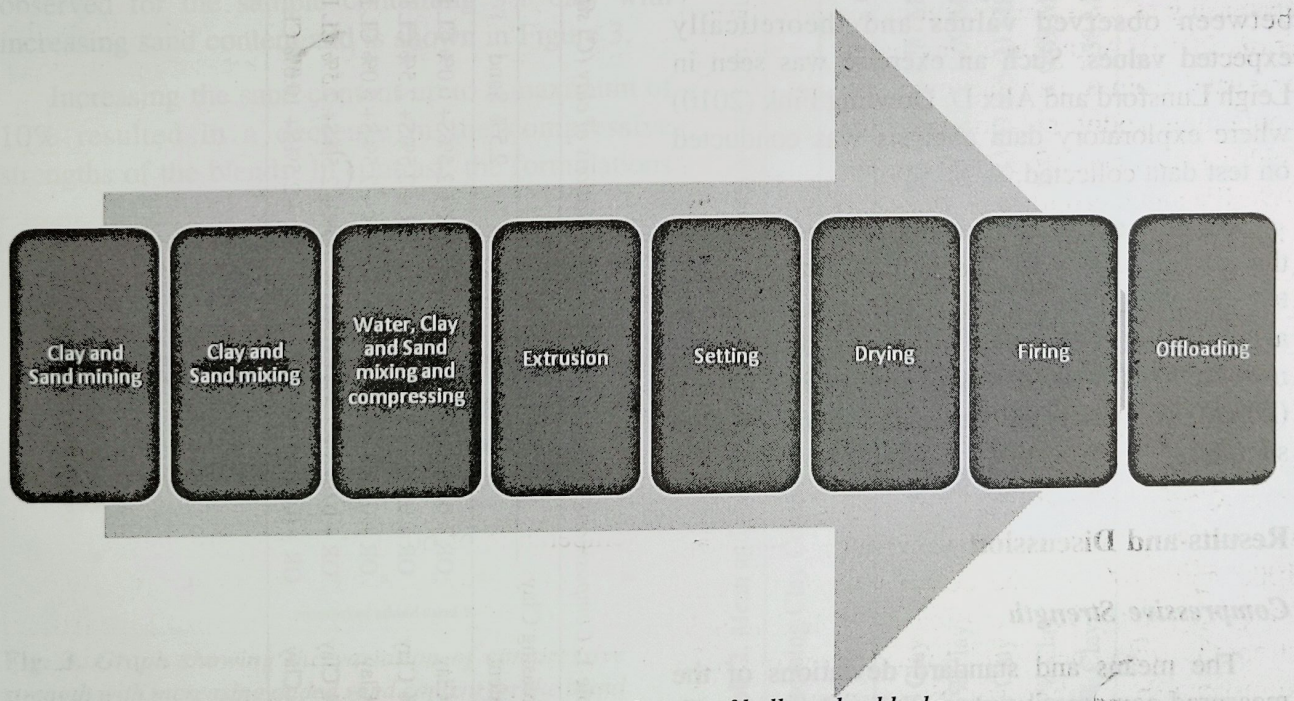

Fig. 1. *Main processes in the manufacture of hollow clay blocks*

The tests were carried out using illuminate condition D65 with observer condition of 2°. The measurements were expressed in CIELAB color space. Precise measurements were repeated using the same sample face in all tests.

Microstructural examination and elemental analysis

A Philips Model 515 Scanning Electron Microscope (SEM) with the Energy Dispersive X-ray Spectroscopy (EDS) attachment was used to examine the microstructure of the fractured surface of the samples. The secondary electron imaging and elemental survey mapping results obtained was automatically recorded and analyzed using Gatan Digscan imaging System. The fractured surfaces of the samples were Gold sputtered for good conductance during analysis. Secondary electrons were captured by the sensor at 30 kV exposure.

Statistical Analysis

Chi square tests as well as paired t-tests were performed. The chi square test or "goodness of fit test" sought to compare the goodness of fit between observed values and theoretically expected values. Such an exercise was seen in Leigh Lunsford and Alix D. Dowling Fink (2010) where exploratory data analysis was conducted on test data collected.

Paired t test is the second method used for the statistical analysis. The paired t-test compares two population means and determines if there is a significant difference in results due to the method. This method was employed in Maharaj (2009b) to verify the quantization of cocaine samples.

Results and Discussion

Compressive Strength

The means and standard deviations of the measured compressive strength for the seven (7)

Table 1. *Compositions of the various blend formulations of clay (C) sand (S).*

Increasing Clay Content	Increasing Sand Content				
	0% Sand	2.5% Sand	5% Sand	7.5% Sand	10% Sand
0% Clay	OR + 0.0%S + 0.0% CL A1	OR + 2.5%S+ 0.0% CL B1	OR + 5.0%S + 0.0% CL C1	OR + 7.5%S+ 0.0% CL D1	OR + 10%S+ 0.0% CL E1
2.5% Clay	OR + 0.0%S + 2.5% CL A2	OR + 2.5%S+ 2.5% CL B2	OR + 5.0%S + 2.5% CL C2	OR + 7.5%S+ 2.5% CL D2	OR + 10%S+ 2.5% CL E2
5% Clay	OR + 0.0%S + 5.0% CL A3	OR + 2.5%S+ 5.0% CL B3	OR + 5.0%S + 5.0% CL C3	OR + 7.5%S+ 5.0% CL D3	OR + 10%S+ 5.0% CL E3
7.5% Clay	OR + 0.0%S + 7.5% CL A4	OR + 2.5%S+ 7.5% CL B4	OR + 5.0%S + 7.5% CL C4	OR + 7.5%S+ 7.5% CL D4	OR + 10%S+ 7.5% CL E4
10% Clay	OR + 0.0%S + 10.0% CL A5	OR + 2.5%S+ 10.0% CL B5	OR + 5.0%S + 10.0% CL C5	OR + 7.5%S+ 10.0% CL D5	OR + 10%S+ 10.0% CL E5

replicates of each of the sample blends tested in accordance with ASTM C67-11 are shown in Table 2 and graphically represented in Figure 2.

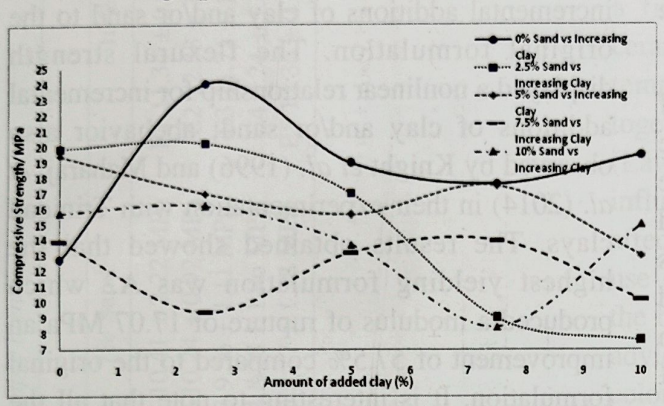

Fig. 2. *Graph showing the variation of compressive strength with increasing clay content for various blends containing different amounts of added sand.*

The non-linear trends obtained for changes in compressive strengths due to the increasing of clay and/or sand content to the original formulation was consistent with observations from similar studies (Davison, 1963; Önal and Sarikaya, 2009; Maharaj, *et al.* 2014). The most linear relationship between compressive strength and formula variation was observed for the sample containing 5% clay with increasing sand content and is shown in Figure 3.

Increasing the sand content up to a maximum of 10% resulted in a decrease in the compressive strengths of the blends. In contrast, the formulations

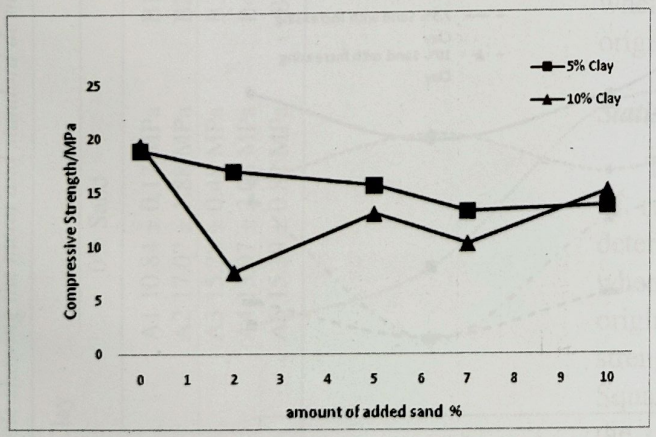

Fig. 3. *Graph showing the variation of compressive strength with increasing added sand content for the blend containing 5% and 10% added clay.*

Table 2. Mean and standard deviations of compressive strength values obtained for various sample blends.

Increasing Clay Content	Increasing Sand Content				
	0% Sand	2.5% Sand	5% Sand	7% Sand	10%Sand
0% Clay	A1 12.7 ± 2.84MPa	B1 19.9 ± 0.96 MPa	C1 19.4 ± 2.73 MPa	D1 13.9 ± 2.42 MPa	E1 15.7 ± 1.45 MPa
2.5%Clay	A2 24 ± 3.17 MPa	B2 20.1 ± 1.69 MPa	C2 16.9 ± 3.69 MPa	D2 9.35 ± 1.33 MPa	E2 16.2± 1.13MPa
5% Clay	A3 18.9 ± 1.84 MPa	B3 17 ± 3.00 MPa	C3 15.6 ± 2.37 MPa	D3 13.2 ± 1.35 MPa	E3 13.7 ± 2.62 MPa
7.5% Clay	A4 17.6 ± 3.23 MPa	B4 9.01 ± 0.69 MPa	C4 17.4 ± 2.97 MPa	D4 14 ± 1.59 MPa	E4 8.45 ± 0.34 MPa
10% Clay	A5 19.4 ± 2.50 MPa	B5 7.57 ± 1.38 MPa	C5 13 ± 2.88 MPa	D5 10.2 ± 1.86 MPa	E5 15 ± 0.00 MPa

with the most variations in compressive strengths were the ones containing 10% added clay with increasing sand content. The non-linearity and fluctuations in compressive strengths for these blends are shown in Figure 3.

With regard to the absolute values of compressive strengths, the lowest compressive strength of 8.45 MPa as obtained for the formulation E4, containing 10% added sand and 7.5% added clay, to the original formula. This represented a decrease of 33% when compared to the original formula. On the other hand, an increase of 2.5% clay without the addition of any sand to the original formula, sample A2, yielded the highest compressive strength which was 24 MPa, representing an increase of 89%. On the basis of compressive strength, sample A2 was found to be the superior formulation.

Modulus of Rupture

The mean and standard deviations of the measured modulus of rupture value of seven (7) replicates for each of the sample blends tested in accordance to ASTM C67-11are shown in Table 3 and a graphical representation of the results shown in Figure 4.

Consistent with the earlier observations of the compressive strength studies, the moduli of rupture (flexural strength) were influenced by the incremental additions of clay and/or sand to the original formulation. The flexural strength displayed a nonlinear relationship for incremental additions of clay and/or sand; abehavior also observed by Knight *et al.* (1996) and Maharaj, *et al.* (2014) in their experimentation with Trinidad clays. The results obtained showed that the highest yielding formulation was A2 which produced a modulus of rupture of 17.07 MPa an improvement of 57.5% compared to the original formulation. It is interesting to note that all the blends containing additional clay but no sand displayed modulus of elasticities values higher than the original blend A1 (>10.84 MPa). On the contrary, the blend with the lowest Modulus of Rupture was E4 with a value of 8.24 MPa. On the basis of Modulus of rupture, sample A2 was found to be the superior formulation.

Colorimetric Analysis

Small color differences were recorded using the ISO 10545-16:1999 method using illuminate condition D65 with observer condition of 2° and the measurements were expressed in CIELAB

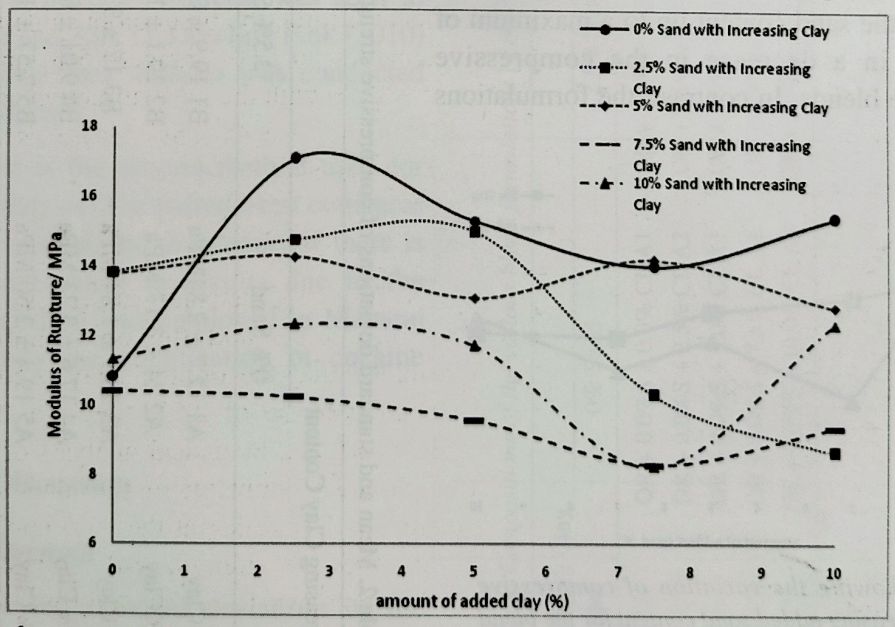

Fig. 4. *Modulus of rupture with increasing clay content for various blends containing different amounts of added sand.*

Table 3. *Table showing the mean and standard deviations of modulus of rupture values obtained for various sample blends.*

Increasing Clay Content	Increasing Sand Content				
	0% Sand	2.5% Sand	5% Sand	7% Sand	10%Sand
0% Clay	A1 10.84 ± 0.17 MPa	B1 13.84 ± 0.22 MPa	C1 13.77 ± 0.88 MPa	D1 10.41 ± 2.22 MPa	E1 11.34 ± 0.94 MPa
2.5%Clay	A2 17.07 ± 1.88 MPa	B2 14.76 ± 1.08 MPa	C2 14.27 ± 1.99 MPa	D2 10.24 ± 0.92 MPa	E2 12.33 ± 1.2 MPa
5% Clay	A3 15.28 ± 0.48 MPa	B3 14.98 ± 1.12 MPa	C3 13.08 ± 0.91 MPa	D3 9.56 ± 1.11 MPa	E3 11.71 ± 1.2 MPa
7.5% Clay	A4 13.97 ± 2.08 MPa	B4 10.30 ± 1.76 MPa	C4 14.18 ± 1.09 MPa	D4 8.28 ± 1.96 MPa	E4 8.24 ± 1.09 MPa
10% Clay	A5 15.39 ± 0.82 MPa	B5 8.65 ± 1.47 MPa	C5 12.83 ± 0.54 MPa	D5 9.37 ± 1.38 MPa	E5 12.36 ± 2.03 MPa

color space which were then translated into actual color for analysis. There is no established color for a fired clay product. Characteristics such as the ceramic clay body formula, kiln atmosphere, firing temperature and various special effects all work together to produce the color of a fired clay body (Lawrence, 1972). By understanding the factors that influence clay body color and knowing how they affect each other, potters can effectively control the use of color in their aesthetic palette. In this case, the best or most attractive color was determined by advice from the manufacturer. The results of the colorimetric analysis are shown in Table 4.

The results clearly demonstrated that variations in colorof the various blends were due to variations in the composition of the mixtures. It can be seen that generally, the darker shades occur for the blends containing higher clay content such as the in the series 10% Clay whereas with increasing sand content,the lighter colorswere observed. To demonstrate this observation, generally lighter colors were observed with samples E1, E2 and E3 which contained 10% sand and less than 5% clay. These became progressively darker as the clay percentage increased (clay content >5%) with sample E5 which contained 10% clay being the darkest. According to the manufacturer, the best colors came from samples containing sand in the range(0-5%) and clay in the range (0-5%) with the most attractive color produced when an increase of 2.5% clay was added to the original formula.

Statistical analysis

The results of the compressive tests, the modulus of rupture tests and the colorimetric analyses determined that the optimal clay product occurred when an increase of 2.5% clay was added to the original formula. Statistical analysis of compressive strength and modulus of rupture data using the Chi Square Test found that at the 95% confidence level, the compressive strength and modulus of rupture test data obtained from the study were independent of the expected data and that the differences between our observed and expected were too great to be

Table 4. *Changes in colours achieved due to variations in clay and sand content.*

Increasing Clay Content	Increasing Sand Content				
	% Sand	2.5% Sand	5% Sand	7% Sand	10% Sand
0% Clay	A1	B1	C1	D1	E1
2.5% Clay	A2	B2	C2	D2	E2
5% Clay	A3	B3	C3	D3	E3
7.5% Clay	A4	B4	C4	D4	E4
10% Clay	A5	B5	C5	D5	E5

explained by chance alone. In this test the critical value calculated using a confidence interval of 95% with 16 degrees of freedom was 26.3 whereas the using the observed data,the chi square statistic was found to be 14.77 (compressive strengths) and 3.96 (modulus of rupture) both less than the critical value.

The paired t-test statistical analysis at the 95% confidence level was used to compare the observed mean for both the compressive strength and modulus of rupture values of the specimen A2 (2.5% addition clay) with those of the original formulation. This test was done by testing two hypothesis. The null hypothesis H_0 stated that the averages were not significantly different whereas the alternative hypothesis H_1 stated that the averages were significantly different. The "calculated p value' was compared to the "chosen p value" and the decision to accept or reject the null hypothesis was made. The test showed that the calculated p values were less than 0.01 for both compressive and modulus of rupture data and the data is shown in Table 5.

Table 5. *Showing statistical parameters and corresponding values for compressive strength and modulus of rupture.*

Parameter	Compressive Strength	Modulus of Rupture
Average Variable 1	23.964	17.053
Average Variable 2	12.704	10.848
Standard Error Variable 1	0.861	0.215
Standard Error Variable 2	0.897	0.084
P value	p<.01	p<.01

The condition for acceptance of the null hypothesis is that the "calculated p value" is greater than the "chosen p value". The results showed that the "calculated p value" was less than the "chosen p value" of 0.05 hence the null hypothesis was rejected. This meant that H_1 was accepted meaning that the averages for the compressive strengths and the modulus of rupture for the sample containing 2.5% added clay were significantly different from those of the unmodified formula. A graphical representation comparing the mean and standard deviations of the compressive strengths and modulus of rupture between the original formulation and the one containing 2.5% added clay error can be seen in Figure 5 and Figure 6 respectively.

The vertical bars seen at the top of the columns represent the variations associated with the repeat sample data in each case. Since in each case the error bars do not overlap, it clearly indicates that there is a significant difference in the compressive strength and the modulus of rupture between formula A2 and the original formula. The graphical representation offers supporting evidence for the statistical analyses that with 95% confidence that A2 significantly different from the original formula in terms of compressive strength and modulus of rupture.

Microstructural Examination and Elemental Analysis

The structure of the ceramic surfaces was investigated using SEM/EDS analysis. The gold coated fractured surfaces were observed at room temperature and Figure 7 shows the results of a

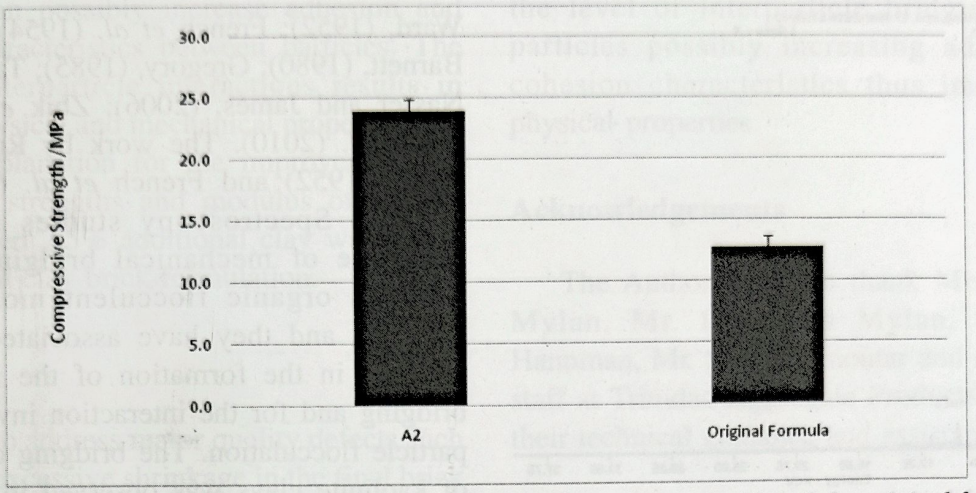

Fig. 5. *Graph representing the Compressive Strength data between formula A2 and the original formulation.*

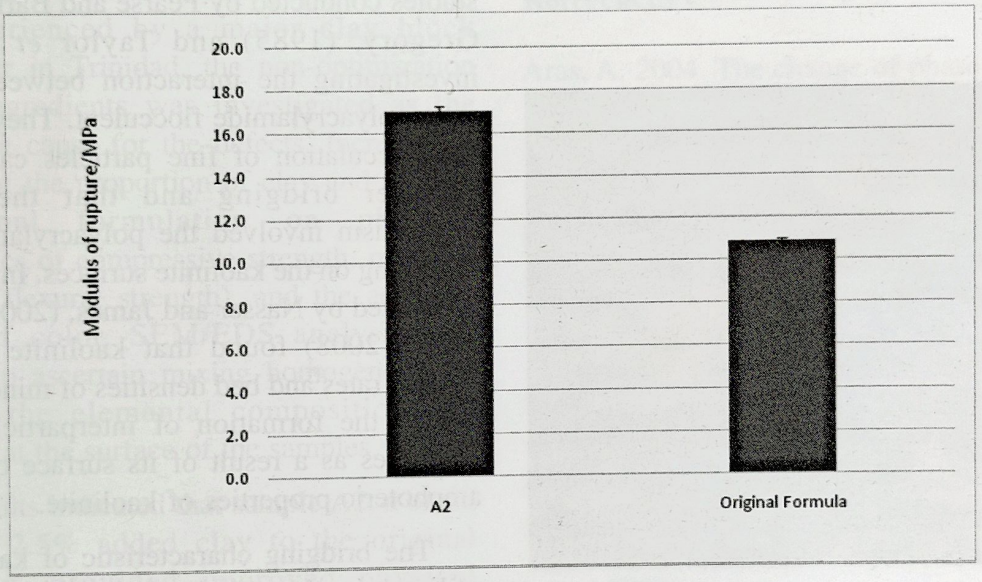

Fig. 6. *Graph representing the Modulus of Rupture data between formula A2 and the original formulation.*

microstructure analysis obtained at the surface of Sample A2 which was typical of the results obtained for the other samples.

The findings are consistent with the results of previous studies by Knight *et al.* (1996) as peaks for Silicon (Si), Oxygen (O), Iron (Fe) and Aluminum (Al) were observed in all the samples tested. The presence of aluminum is indicative of the presence of kaolinite (Maharaj 2009a). The chemical structure of kaolinite is $Al_2Si_2O_5(OH)_4$ with a typical composition of 39.8% aluminum oxide, 46.3% silica, and 13.9% water. It is a layered silicate mineral, with one SiO_4 tetrahedral sheet linked through oxygen atoms to one octahedral sheet of alumina octahedra (Deer *et al.* 1992). The energy dispersive x-ray analysis system (EDS) was used to investigate the distribution of the elements at the surface of the samples and the elemental mapping for aluminum is shown in Figure 8. The elemental map for the Aluminum very closely resembled (with respect to the dark regions) the map of the gold that was used for gold sputtering of the samples. It could be concluded that the dark regions were due to the

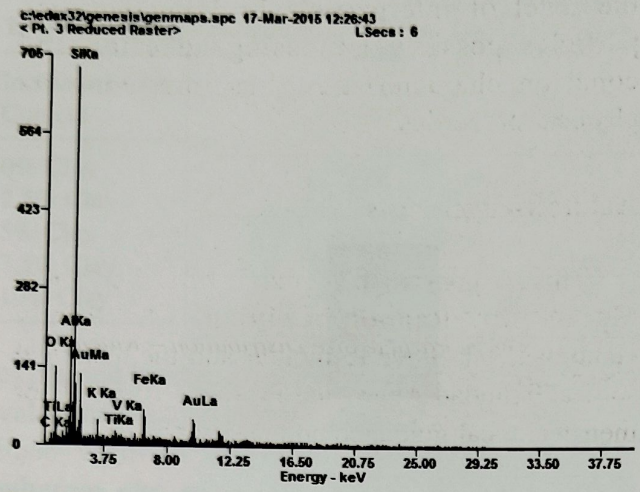

Fig. 7. *Microstructure analysis at the surface of Sample A2.*

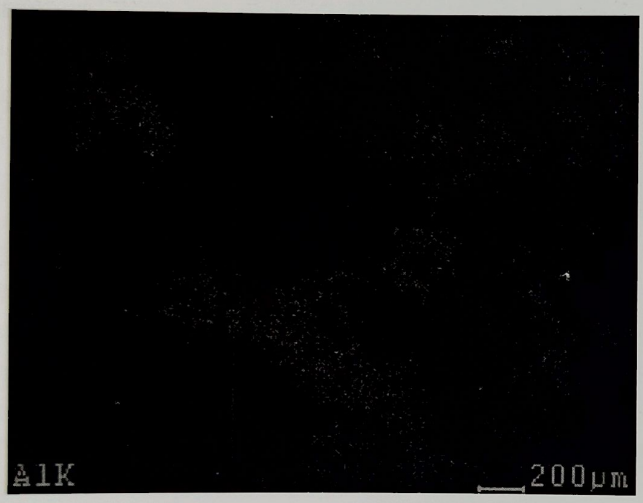

Fig. 8. *The energy dispersive x-ray mapping for aluminium for sample A2*

detector not being able to receive any x-rays at those regions due to the morphology of the fractured surface. With the exception of the dark regions, the distribution of the Aluminum was homogenous and this indicates that there was thorough mixing during the preparation of the various blends.

Thepresence of kaolinite is significant as there exists strong evidence to support the suggestion that kaolinite clays participate in inter-particle bridging in composite systems (Wadsworth and Cutler, (1956); Ruehriven and Ward, (1952); French *et al.* (1954); Pearse and Barnett, (1980); Gregory, (1985); Taylor, (2002); Nasser and James, (2006); Zbik *et al.* (2008); Du *et al.* (2010). The work by Ruehriven and Ward, (1952) and French *et al.* (1954) using Infrared Spectroscopy studies showed the existence of mechanical bridging networks between organic flocculent molecules and kaolinite and they have associated hydrogen-bonding in the formation of the inter-particle bridging and for the interaction involved in the particle flocculation. The bridging characteristic of kaolinite clays was observed in flocculation studies conducted by Pearse and Barnett, (1980), Gregory, (1985) and Taylor *et al.* (2002) investigating the interaction between kaolinite anda polyacrylamide flocculent. They found that the flocculation of fine particles can occur by polymer bridging and that the bridging mechanism involved the polyacrylamide chains absorbing on the kaolinite surfaces. Investigations conducted by Nasser and James, (2006) and Zbik *et al.* (2008) found that kaolinite influenced settling rates and bed densities of mineral tailings due to the formation of interparticle bridging structures as a result of its surface charges and amphoteric properties of kaolinite.

The bridging characteristic of kaolinite was utilized in the reinforcement of natural and synthetic elastomers (Theng, 1970) as the blending of kaolinite to the polymer matrix during vulcanization results in the formation of crosslinked polymer-clay networks with the resulting material showing significant improvements in the bulk modulus and abrasion resistance compared with unmodified polymeric materials. The bridging/aggregation properties of kaolinite materials have been recently utilized industrially by Du *et al.* (2010) who showed that well crystallized kaolinites facilitated effective bridging flocculation as applied to solid/liquid. Although the exact nature of the interaction of the kaolinite within the ceramic material system remains unclear, it's bridging/aggregation

properties can possibly increase adhesion and cohesion characteristics between particles. The improved interparticle interactions results in improved physical and mechanical properties and offers an explanation for the improvements in compressive strengths and modulus of rupture observed when 2.5% additional clay was added to the original clay brick formulation.

Conclusion

In order to address major quality defects such as cracking, excessive shrinkage in the final brick product as well as unsatisfactory product color being experienced by a major clay block manufacturer in Trinidad, the non-optimization of block ingredients was investigated as the possible root cause for the defects. Incremental deviations of the proportion of clay and sand to the original formulation on physical characteristics of compressive strength, modulus of rupture (flexural strength), and the aesthetic property of color. SEM/EDS analysis was conducted to ascertain mixing homogeneity by observing the elemental composition and distribution at the surface of the samples.

The results indicated that sample A2, a blend containing 2.5% added clay to the original formulation, provided improved physical properties compared to the original sample in the following manner:

- An increase in compressive strength value of 89%.
- An increase in the modulus of rupture (flexural strength) value of 58%.
- An improvement in the colour aesthetic.

The results of the SEM and elemental mapping at the surface of the ceramic materials showed the presence of aluminum atoms (from the clay material as kaolinite) homogenously dispersed. This indicated that the mixing process was efficient. The added clay (kaolinite) played a role within the ceramic material by increasing the level of interparticle bridging between particles possibly increasing adhesion and cohesion characteristics thus improving its physical properties.

Acknowledgements

The Authors wish to thank Mrs. Poorandai Mylan, Mr. Randolph Mylan, Mr. Randy Hanuman, Mr. Steve Ramoutar and the technical staff at Trinidad Aggregate Products Limited for their technical guidance and assistance.

References

Aras, A. 2004. The change of phase composition in kaolinite- and illite-rich clay-based ceramic bodies. *Applied Clay Science*. **24**: 257-269.

Fernanda, A., Castellini, E., Manfredini, T. and Romagnoli, E. 2004. The role of sodium hexametaphosphate in the dissolution process of kaolinite and kaolin. *Journal of the European Ceramic Society*. **24** (7) : 2113-2124.

AS 4459.16 (2005) Methods of sampling and testing ceramic tiles - Determination of small colour differences. (ISO 10545-16:1999 MOD)

ASTM C67-11, Standard Test Methods for Sampling and Testing Brick and Structural Clay Tile, ASTM International, West Conshohocken, PA, 2011, www.astm.org

Davison, J.I. 1963. Properties of clay bricks manufactured in the Atlantic Provinces. Ottawa: National Research Council Canada, Division of Building Research.

Deer, W.A., Howie, R.A., Zussman, J. 1992. An introduction to the rock-forming minerals (2 Ed.). Harlow: Longman.

Du, J., Morris, G., Pushkarovar, R.A. and St. C. Smart, R. 2010. Effect of Surface Structure

of kaolinite on aggregation, settling rate and bed density. *Langmuir.* **26**(16) : 13227–13235

French, R.O., Cook, M.A., Wadsworth, E.M. and Cutler, B.I. 1954. The qualitative application of infrared spectroscopy to studies in surface chemistry. *Journal of Physical Chemistry.* **54**: 805.

Gregory, J. 1985. The use of polymeric flocculants. *Proceedings of the Engineering Foundation Conferences on flocculation, sedimentation and consolidation*. American Institute of Chemical Engineers, New York, USA, pp. 253–263.

Guggenheim, S. and Martin, R. T. 1995. Definition of clay and clay mineral: Joint report of the AIPEA nomenclature and CMS nomenclature committees. *Clay and Clay Minerals.* **43** (2) : 255-256.

Knight, J.C. 1996. Ceramic potential of some Trinidad clays: 2. Fired characteristics. *British Ceramic Transactions.* **95**(4) : 162-168.

Knight, J.C ., Grierson, and Hosein, A. 1996. Ceramic potential of some Trinidad clays: 1 Chemistry and mineralogy. *British Ceramic Transactions.* **95** (3).

Knight, J.C. and Hosein, A. 1997. Ceramic characteristics of the white burning Valencia clay of Trinidad. *West Indian Journal of Engineering*. **20** : 76-84.

Lawrence, W.G. Ceramic Science for the Potter, Chilton Book Co., 1972, pp. 35 : 119-120.

Lunsford, L. and Fink, A.D.D. 2010. Water taste test data. *Journal of Statistics Education.* **18** (1)

Maharaj, R. 2009a. Composition and Rheological properties of Trinidad Lake Asphalt and Trinidad petroleum bitumen. *International Journal of Applied Chemistry*. **5** (3) : 169-179.

Maharaj, R. 2009b. Quantitative analysis of cocaine using Fourier transform infra-red spectroscopy-attenuated total reflectance: A preliminary investigation. *Internet Journal of Third World Medicine*. **7** (2) : 3

Maharaj, R., Maharaj, C., White, D., Penjilia C. and Ramlagan, S. 2014. Optimization of ingredients for clay block manufacturer: Unfired characteristics. *Trends in Applied Sciences Research.* **9** : 574-587.

Maskel, D., Heath, A. and Walker, P. 2013. Laboratory scale testing of extruded earth masonryunits. *Materials and Design.* **45**: 359-364.

Murray, H.H. 2000. Clays. Ullmann's Encyclopedia of industrial chemistry, 6th Edition. Wiley-VCH Verlag Gm BH, Weinheim, Germany, pp30.

Nasser, M.S. and James, A.E. 2006. Settling and sediment bed behavior of kaolinite in aqueous media. *Separation and Purification Technology.* **51**(1) : 10-17.

Önal, M. and Sarikaya. Y. 2009. Some physicochemical properties of a clay containing smectite and polygorskite. *Applied Clay Science*, **44** (1-2), 161-165.

Pearse, M.J. and Barnett, J. 1980. Chemical treatments for thickening and filtration. *Filtration and Separation.* **17**(5) : 465-470

Possehl, G.L. 2002. The Indus civilization: A contemporary perspective. Rowman Altamira, Walnut Creek, CA., pp 276.

Punmia, B.C. and Jain, A.K. 2003. Basic civil engineering. Firewall Media, New Delhi, India. pp 446.

Pusch, R. 2006. Mechanical properties of clays and clay minerals. In Handbook of Clay Science, edited by F. Bergaya, BKG Theng and G. Lagaly. Sweden: Elsevier Ltd.

Ramdath, H. 2012. Exploitation of mineral resources - Trinidad and Tobago 2011 [cited June 2012]. http://www.energy.gov.tt/content/241.pdf. (accessed 22.04.2015)

Ruehrwein, R.A.and Ward, D.W. 1952. Mechanisms of clay aggregation by polyelectrolytes. *Soli Science*. **73** : 485-492.

Taylor, M.L., Morris, G.E., Self, P.G. and Smart, R.S.C. 2002. Kinetics of adsorption of high molecular weight anionic polyacrylamide onto kaolinite: The flocculation process. *Journal of Colloid and Interface Science*. **250**(1) : 28-36.

Theng, B. K. G. 1970. Interactions of clay minerals with organic polymers some practical applications. *Clays and Clay Minerals*. **18** : 357-362.

Wadsworth, E.M. and Cutler, B.I. 1956. Flocculation of mineral suspensions with coprecipitated polyelectrolytes. *Mining Engineering*. **205**: 830-833.

Zbik, M., Smart, R. and Morris, G. 2008. Kaolinite flocculation structure. *Journal of Colloid and Interface Science*. **328**(1) : 73-80.

(Received March,2017; Accepted May 2017)

Clay Research, Vol. 35, No. 2, pp. 84-90 (2016)

Method of Identification of Bentonite for Industrial Application

ABDUL RAHMAN GADA* AND SMITHA YADAV

National Institute of Construction Management and Research, Pune 411045

Abstract–*Bentonite is naturally occurring clay predominantly composed of smectite minerals. The main uses of bentonite are for drilling mud, binder, absorbent, purifier and as ground water barrier. The total resources of Bentonite in India as per UNFC system as on 2010 are about 568 million tonnes occurring predominantly in Rajasthan and Gujarat. Bentonite exhibits various properties such as swelling, high surface area, high liquid limit; which varies from source to source. Thus their testing before put to any application becomes necessary. In this work, a methodology of identification of bentonite is specified which highlights quick and easier identification of the material and its use in industrial application without taking the research to microscopic level of examination.*

Key words : Atterberg Limits, Chemical Industry, Swelling, X – Ray Diffraction (XRD) and Smectite.

Introduction

Bentonite are smectite rich clays irrespective of their origin. They exhibit properties like high swelling, high surface area, good viscosity, high liquid limit, thixotropy, colloidal and water proofing, binding, impermeability, plasticity, tendency to re-act with organic compounds and cation exchange capacity (CEC). As a result of which they have applications in construction activities like in drilling mud, slurry walls, ground water barrier, water treatment, grouting and industrial applications like iron ore and animal and poultry feed pelletization, paints, cosmetics and pharmaceuticals, as foundry sand bonding material, ceramics etc. However, the use of the material may differ due to the properties it may exhibit which depends on the source of origin. This paper addresses the methodology of identification without taking recourse to the microscopic level of examination. Bentonite consists predominantly of smectite minerals having various exchangeable ions . The exchangeable ions include Mg^{++}, Ca^{++}, Na^{+}, Fe^{++}, Zn^{++} and Li^{+} (Inglethorpe *et al.,* 1993. Table 1 shows resources of bentonite across different states in India. Carlson (2004) carried out characterization of bentonite from 5 regions around the world namely Wyoming (USA), Kutch (Gujarat, India), Milos (Greece), Neubrandenburg (NE Germany) and four localities in Czech Republic. In her report, the emphasis was to determine crystal structure and chemical composition of clay minerals. The research employed methods like X – Ray Diffraction (XRD), differential thermal analysis (DTA), Fourier transform infrared spectroscopy (FTIR), transmission electron microscopy (TEM), and scanning electron microscopy (SEM). Olsson *et al.,* (2009) carried out characterization of Kutch (India) and Milos (Greece) bentonite to test their suitability for use as tunnel back – fill material. However, the research required tests like grain-size analyses, aqueous leachates, determination of free iron oxides, cation exchange capacity (CEC) and exchangeable cations and X-ray diffraction analysis (XRD) for the identification. Asad *et al.,* (2013) in his research work carried out characterization of bentonite clay of Dhaka (Bangladesh), China and Pakistan for its

***Corresponding Author Email :** abdulgada@gmail.com

suitability based on cost. The research emphasized on employing geotechnical tests, specific gravity, Atterberg limits, and grain size distribution. However, the research was not proper to convey the suitability of the samples in any industrial or construction industry and hence confining itself only to characterization. This work thus tries to address the issue of characterization as well as finding its suitability in industrial application

Materials and Methods

Gujarat since being a major resource of Bentonite as shown in table 1, the samples for the work analysis were procured from Bhavnagar and Kutch. Bhavnagar and Kutch were primarily selected as three fourth of the deposits of bentonite were found in this region. In order to determine geotechnical properties of bentonite, various tests were performed complying with the relevant standards like natural moisture content determination (IS 2720 Part 2: 1973), specific gravity (IS 2720 – Part 3), liquid limit and plastic limit (IS 2720 – Part 5), shrinkage limit (IS 2720 – Part 6), grain size analysis (IS 2720 – Part 4), swelling pressure (IS 2720 – Part 41), free swell index (IS 2720 – Part 40), water content- dry density relation (IS 2720 – Part 7), pH value (IS 2720 – Part 26). Three specimens were tested under each of the tests specified and the average of the readings was taken for analysis. To determine the mineralogical composition of bentonite X-Ray diffraction (XRD) was undertaken. The spectrum was fed in software to determine mineralogical composition and the percentage of various minerals present.

Results and discussion

The results of the various tests were given below in table 2 with their corresponding graphs and figures attached. The various Industrial applications of Bentonite are listed below.

Table 2. *Results of various Experimental studies*

Properties	Bhavnagar	Kutch
Natural Moisture Content	7.23	3.27
Specific Gravity	2.167	2.222
Liquid Limit – Casagrande	92	102
Liquid Limit – Cone Penetration	86	36
Plastic Limit	47.13%	57.08%
Shrinkage Limit	7.38	-
Soil Classification	CH	CH
Swelling Pressure	0.607	0.0568
Free Swell Index	463.33	183.33
Standard Proctor Test	1.48	1.22
MDD (gm/cc)	19.6	35.5
OMC (%)		
pH	7.85	8.87

Foundry

In foundries use green sand for casting metal which is a mixture of sand, bentonite, clay and water. Bentonite in this case acts as a binder. The quality of bentonite thus needs to be known

Table 1. *Reserves/Resources of Bentonite as on 1.4.2010 (By States)*

(In tonnes)

State	Reserves (A)	Remaining Resource					Total (B)	Total (A+B)
		Pre-feasibility	Measured	Indicated	Inferred	Recon-naissance		
Gujarat	12460170	-	2163813	1904	119553173	-	121718890	134179060
Jammu & Kashmir	-	-	-	-	147400	-	147400	147400
Jharkhand	609406	3067	-	-	367527	-	370594	980000
Rajasthan	11990932	-	24356005	222017000	139423096	25730000	411526101	423517033
Tamil Nadu	-	-	-	3725333	5818519	-	9543852	9543852

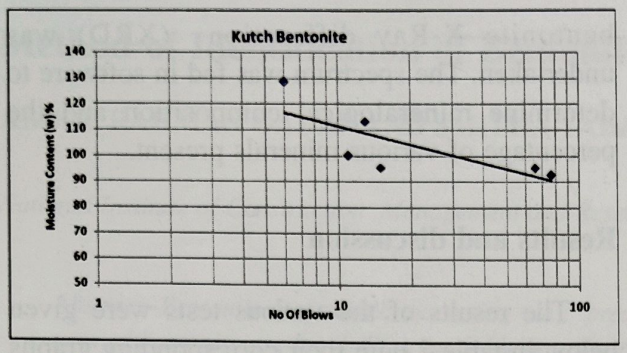

Fig. 1. *Casagrande's Method – Kutch Bentonite.*

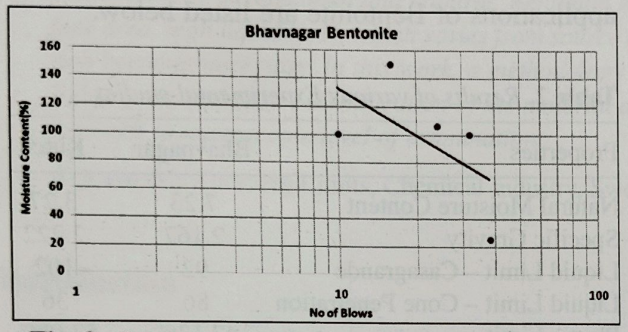

Fig. 2. *Casagrande's Method – Bhavnagar Bentonite*

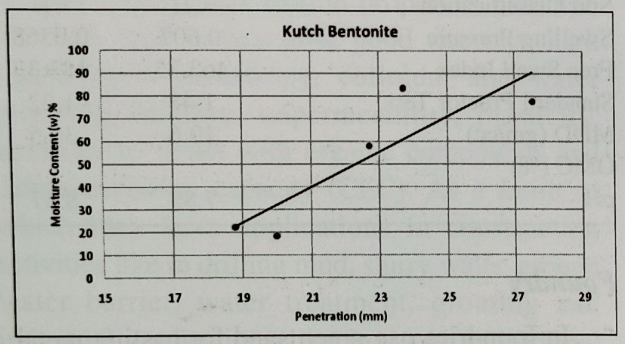

Fig. 3. *Cone Penetration Method – Kutch Bentonite*

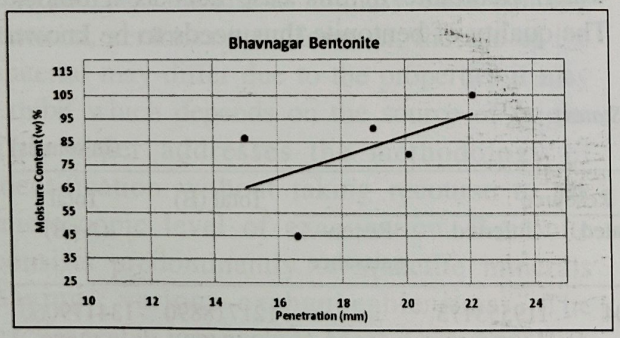

Fig 4. *Cone Penetration Method – Bhavnagar Bentonite.*

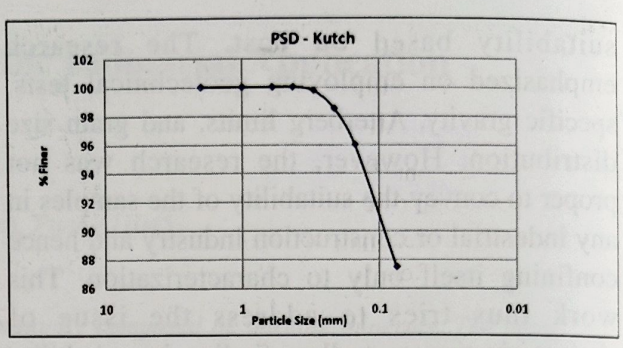

Fig. 5. *Particle Size Distribution – Kutch.*

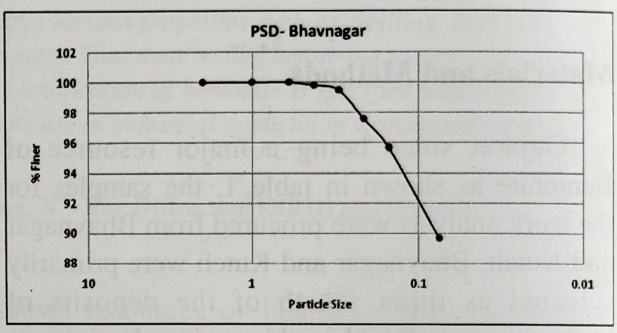

Fig. 6. *Particle Size Distribution – Bhavnagar.*

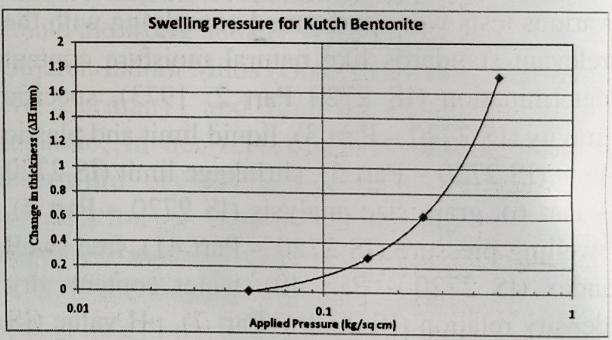

Fig. 7. *Swelling Pressure – Kutch*

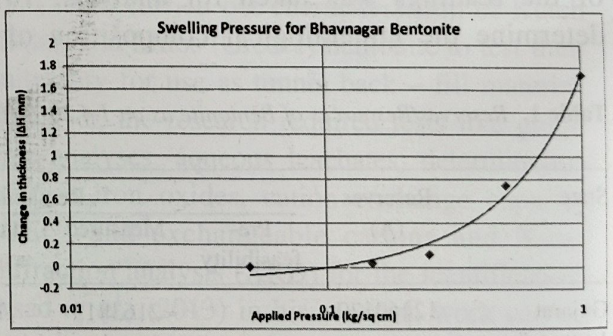

Fig. 8. *Swelling pressure - Bhavnagar.*

Table 3. *Properties of Suitability of Bentonite in Foundry*

Sr. No.	Properties	Typical Value	Obtained Value	
			Bhavnagar	Kutch
1.	Moisture Content (%)	6 – 18	7.653	3.973
2.	Liquid Limit (%)	600 – 800	92	102
3.	Swelling Index	>25	74.5	12
4.	Fineness – Retained on 125 μ sieve (%)	3	6.3	7.17
5.	CEC (meq of MB/100g of bentonite)	98	ND*	ND*

*ND: Not determined

prior to its use. IS 12446:2007 prescribes the various essential properties to be present in bentonite for its application in the foundry. The comparison of the same with Bhavnagar and Kutch samples is shown in table 3.

Grouting of low grade

Bentonite is used as a substitute in specific proportions in the cement grout. The addition of bentonite in the grout decreases the setting time of cement and forms a homogeneous colloidal mix. IS 12584: 1989 specifies the requirements of bentonite to be used in grouting. The comparison of the same with the tested samples is shown in table 4.

Table 4. *Properties of Suitability of Bentonite in Grouting.*

Sr. No.	Properties	Typical Value	Obtained Value	
			Bhavnagar	Kutch
1.	Liquid Limit (%)	>100	92	102
2.	Swelling	4 – 6 times	5.6	2.83
3.	pH	>7.5	7.85	8.87

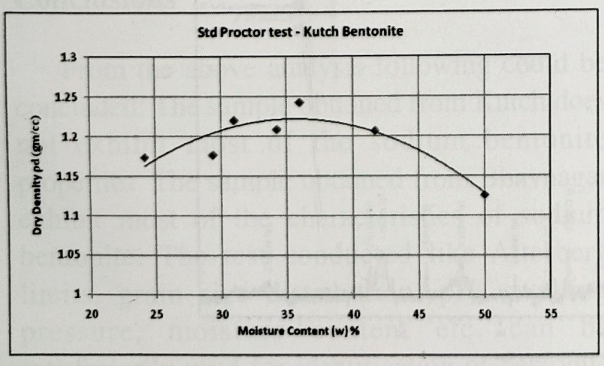

Fig. 9. *Standard Procter Test – Kutch Bentonite*

Bentonite as Bleaching Agent

Bleaching agents require acid activation of material which is attained at low pH value. Pigments are captured by donation H^+ ions which are achieved by large surface areas. Table 5 shows the requirements of bentonite for its suitability as bleaching agent and also compares the properties exhibited by both the tested samples.

Bentonite in Ceramics Industry

Bentonite is used in ceramics industry to modify flow properties of glazes and as plasticizers which aids in formation of ceramic bodies. IS 12621: 1988 specifies the requirements of bentonite to be used in ceramic industry. The comparison of these requirements with the tested samples is shown in table 6.

Bentonite in Drilling Mud

Bentonite produces highly viscous slurry which exhibit thixotropic properties. Thus, bentonite acts as a suspending agents which could be used as a drilling fluid in Industrial application.

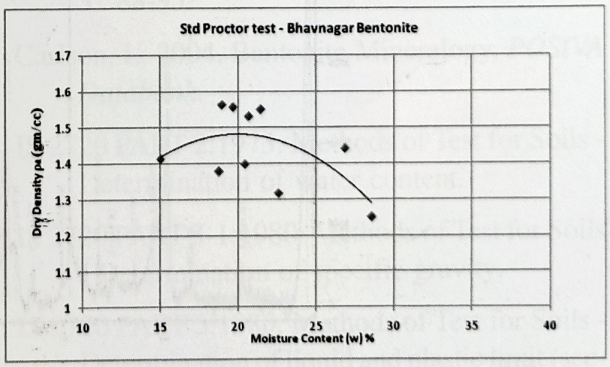

Fig. 10. Standard Procter Test – Bhavnagar Bentonite

Table 5. *Properties of Suitability of bentonite as Bleaching agent.*

Sr. No.	Property	Typical Value	Obtained Value	
			Bhavnagar	Kutch
1.	Free Swell Capacity	<12	5.6	2.83
2.	pH value	2.5 – 3	7.85	8.87
3.	Moisture content (%)	<12	7.653	3.973
4.	Montmorillonite content (%)	>=50	48.6	26.4

Table 6. *Properties of Suitability of bentonite in Ceramics Industry.*

Sr. No.	Property	Typical Value	Obtained Value	
			Bhavnagar	Kutch
1.	Swelling Power	15 – 20	74.5	24
2.	Moisture Content	6	7.653	3.973
3.	Fineness – Retained on 125 μ sieve (%)	0	7.82	9.57
4.	Viscosity at 30°C, centipoise, Min	4.5	ND*	ND*
5.	Plastic Limit	45 – 60	47.13%	57.08%

*ND: Not determined

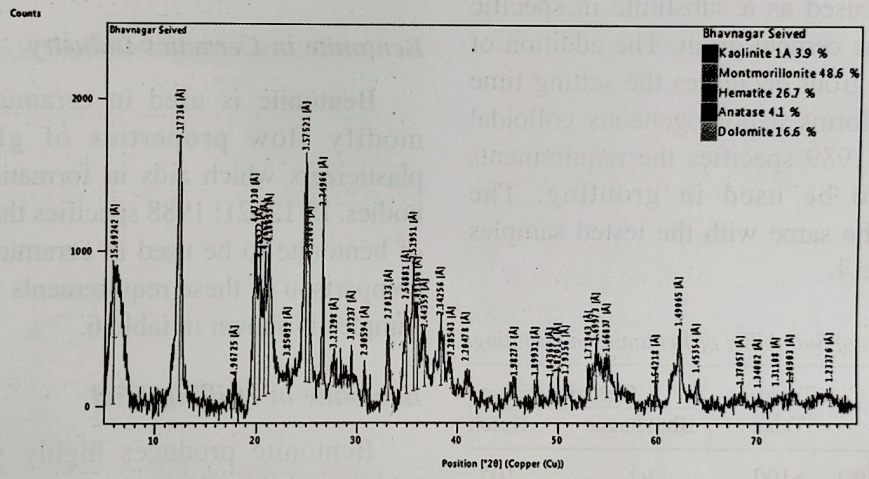

Fig. 11. *X – Ray Diffraction test – Bhavnagar.*

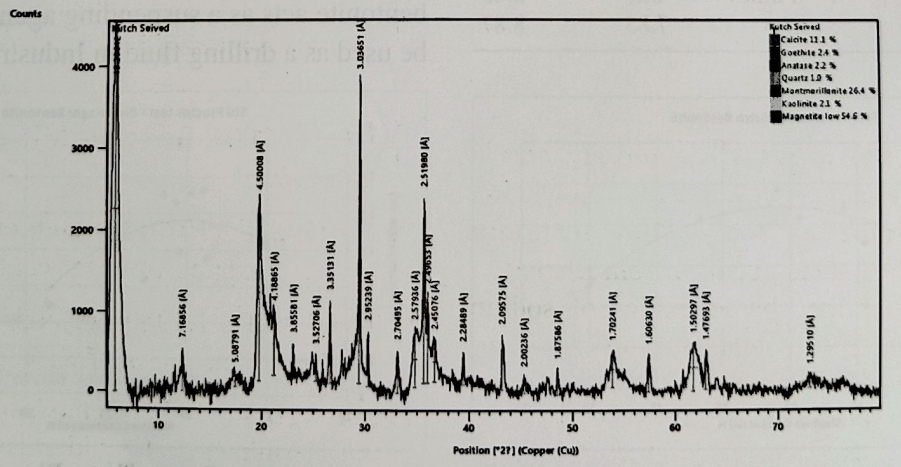

Fig. 12. *X – Ray Diffraction test – Kutch.*

Table 7. *Properties of Suitability of bentonite in Drilling Mud.*

Sr. No.	Property	Typical Value	Obtained Value	
			Bhavnagar	Kutch
1.	Moisture Content (%)	>=12	7.653	3.973
2.	Sand Content (%)	2	10.3	12.5
3.	Fineness (Dry)To pass through 150-μ IS Sieve, (%) by mass, Min	98	95.7	96.0
4.	Fineness (Dry)To pass through 75 – μ IS sieve, (%) by mass, Min	90	89.7	86.5

Table 8. *Properties of Suitability of bentonite in Chemical and Petroleum Industry*

Sr. No.	Property	Typical Value	Obtained Value	
			Bhavnagar	Kutch
1.	Moisture Content (%)	5 – 12	7.653	3.973
2.	Fineness (Dry) To pass through 75 – μ IS sieve, (%) by mass, Min	95	89.7	86.5
3.	pH	9 – 10.5	7.85	8.87

Table 7, shows requirements of bentonite for its suitability as drilling mud. The Bhavnagar and Kutch samples are compared with these requirements.in the same table.

Bentonite in Chemical Industry and Decolourising of Petroleum and Vegetable oils

Bentonite is used as catalyst for chemical production and pharmaceutical industry. pH value and large surface area help in colour pigment removal of petroleum and vegetable oils. IS 6186:1986 specifies requirements of bentonite for putting it into use for various industrial activities. Comparison of these requirements with both samples are undertaken in Table 8.

Conclusions

From the above analysis following could be concluded: The sample obtained from Kutch does not exhibit most of the sodium bentonite properties. The sample obtained from Bhavnagar exhibit most of the characteristics of sodium bentonite. The test conducted like Atterberg limits, grain size distribution, pH, swelling pressure, moisture content etc. can be satisfactorily used for identification of bentonite without making use of laborious and cumbersome microscopic analysis.XRD test confirms presence of smectite group minerals in both the samples with its constituent more than 50% in Bhavnagar sample. The Bhavnagar and Kutch Bentonite can be used in 1) Chemical industry and decolourising of petroleum and vegetable oils 2) Low grade grouting.

References

Asad, Md. Abdullah , Shantanu Kar, Mohammad Ahmeduzzaman, Md. Raquibul Hassan. 2013. Suitability of Bentonite Clay: An Analytical Approach.

International Journal of Earth Science. Vol. 2, No. **3** : 88-95.

Carlson, L. 2004. Bentonite Mineralogy, *POSIVA Databank.*

IS 2720 PART 2:1973: Methods of Test for Soils - Determination of water content.

IS 2720 PART 3-1:1980: Methods of Test for Soils - Determination of specific gravity.

IS 2720 PART 5:1985: Methods of Test for Soils - Determination of liquid and plastic limit (second revision).

IS 2720 PART 6:1972: Methodsof Test for Soils - Determination of shrinkage factors (first revision).

IS 2720 PART 4:1985: Methods of Test for Soils - Grain size analysis (second revision).

IS 2720 PART 41:1977: Methods of Test for Soils- Measurement of swelling pressure of soils.

IS 2720 PART 40:1977: Methods of Test for Soils - Determination of free swell index of soils.

IS 2720 PART 7:1980: Methods of Test for Soils - Determination of water content-dry density relation using light compaction (second revision).

IS 2720 PART 26:1987: Methods of Test for Soils - Determination of pH value.

IS 12446: 2007: Bentonite for Use in Foundries – Specification.

IS 12584: 1989: Bentonite for Grouting in Civil Engineering Works – Specification.

IS 6186: 1986: Specification for Bentonite.

IS 12621: 1988: Bentonite for Ceramic Industry – Specification.

Indian Minerals Yearbook 2013 (Part III: Mineral Reviews) – Indian Bureau of Mines.

Inglethorpe, S.D.J., Morgan, D.J., Highley, D.E. and Bloodworth, A.J. 1993. Industrial Minerals Laboratory Manual Bentonite, *British Geological Survey,* WG/93/20, 1 – 116.

Olsson, S, Ola Karnland, Dec 2009. Characterisation of bentonites from Kutch, India and Milos, Greece – some candidate tunnel back-fill materials, *ISSN*, (R–09–53), 0-35.

(Received March, 2017; Accepted June, 2017)

Clay Research, Vol. 35, No. 2, pp. 91-108 (2016)

Re-search Shrink-Swell Measurement and Relationship with Soil Properties of Black Clayey Tropical Vertisols

PRAVIN B. THAKUR[A*], TAPAS BHATTACHARYYA[B], S. K. RAY[C], P. CHANDRAN[D], D. K. PAL[D] AND B. A. TELPANDE[D]

[A]ICAR-Central Research Institute for Dryland Agriculture, Hyderabad-500 059
[B]Dr. Balasaheb Savant Konkan Krishi Vidyapeeth, Dapoli- 415 712
[C]ICAR-National Bureau of Soil Survey and Land Use Planning, Jorhat-785 004
[D]ICAR-National Bureau of Soil Survey and Land Use Planning, Nagpur-440 033

Abstract–*Shrink–swell phenomenon is a complex process in vertic group of soils. Their dynamics in soils has long been presented through various models, field and laboratory methods. The present study finds out a feasible way to measure the shrink-swell potential and the key responsible factors in soil which are most influential in determining this phenomenon. Four shrink– swell parameters such as coefficient of linear extensibility (COLE), coefficient of linear shrinkage (COLS), percent volume change on swelling (PVCsw), percent volume change on shrinkage (PVCs) measured at 25°C (room temperature,RT), 40°C and 110°C were used to quantify shrink – swell phenomenon. Results indicated that heating the soil cake at 110°C over 40°C does not bring higher change (0-10 %) in linear shrinkage, the corresponding value for volume change at 110°C showed greater change (3-61%) hence, COLS at 40°C and PVCs at 110°C amongst others were promising and may be recommended for routine measurement of shrink–swell phenomenon in the laboratory. Out of three the different measurement devices, cube shaped box appeared to be the better option. The soil properties which represent carbon content and soil substrate have significant correlations ($p<0.01$, $p<0.05$) with the corresponding shrink–swell parameters. The multiple regression analysis showed 69 percent variation for PVCs 110°C and 63 percent for COLS 40°C.*

Key words : Hysteresis, Shrink-swell, Volume change, Exchangeable cations, Carbon

Vertisols and their intergrades are recognized for high natural fertility and suitability for agriculture (Acquaye *et al.,* 1992). These soils are distinct due to their colour, cracks and, shrink–swell nature which severely limit utilization of these Vertisols.

Understanding the shrink – swell behaviour of Vertisols is important. Intricacy in intrinsic soil properties, climate and other (management) factors, and their interactions needs to be assessed. Smectite is a dominant clay mineral present in Vertisols and is more responsible for swelling and shrinkage even if, it is present in small amount (Bhattacharyya *et al.,* 1993; 1997). Later, it is reported that minimum 20 percent smectite may bring the observed swelling and shrinkage in field (Shirsath *et al.,* 2000). In this way other soil parameters such as water content, clay content, types of cations present, structure, oxides of Al^{+} and/or Fe^{2+}, soil organic matter, compaction and density are widely reported to contribute to this unusual phenomenon in various literatures (Davidson *et al.,* 1956; Franzmeier and Ross, 1968; Grossman *et al.,* 1968; Anderson *et al.,* 1973; McCormack *et al.,* 1975; Smith *et al.,* 1985; Thomas *et al.,*2000; Bhuse *et al.,* 2001; Igwe *et al.,* 2003; Bovine *et al.,* 2009). Most of the Vertisols are calcareous and the development of calcareousness causes the enhancement in

***Corresponding Author Email :** pravin_lrmstudent99@yahoo.co.in^X ^; tapas11156@yahoo.com**

exchangeable Mg^{2+} and Na^{+}. Therefore, the relation between shrink – swell and other properties *viz.*, $CaCO_3$, exchangeable sodium percentage (ESP) and exchangeable magnesium percentage (EMP) (Balpande *et al.*, 1996; Kadu *et al.*, 2003) should also be considered. Elsewhere, it has been reported that soil inorganic carbon ($CaCO_3$) reduces shrinkage (Rimmer and Greenland, 1976). Since, this has a direct relation with crop performance in these Vertisols; it demands quantification of shrink-swell phenomenon.

The shrink – swell can be quantified through coefficient of linear extensibility (COLE) or a potential volume change (PVC or swell index). Numerous methods have been proposed in the past to measure shrink –swell potential of expansive soils (Franzmeier and Ross, 1968; Grossman *et al.*, 1968; Yule *et al.*, 1980; Schaffer and Singer, 1976; Ross, 1978; Groenevelt and Grant, 2004; Mckenzie *et al.*, 1994). Of that,soil paste ($COLE_{rod}$) technique (Schaffer and Singer, 1976) is commonly followed in the laboratory studies. Although, necessitating suitable method to measure shrink – swell potential (Nayak *et al.*, 2006; Qi *et al.*, 2011) and may provide rational predictability from laboratory to field (Dinka and Lascano, 2012).

The COLE is a uni-directional (linear) measurement of shrink – swell potential of soils. The method postulated by Schaffer and Singer's (1976) suggests that COLE is to be measured by change in linear shrinkage over moist value. This method as such, therefore, measures coefficient of linear shrinkage (COLS) and not the COLE as suggested by these authors. Besides, since soil is a three dimensional object, measurement of shrink – swell in one direction may not give a true picture. Thus, measurement of the volume change may be a useful parameter to find out the extent of shrink – swell in black soils. Very little information is available about temperature effects on soil drying whether soil should dry in normal room temperature (Schaffer and Singer, 1976) or oven dry as defined by Soil Survey Staff (2014). Moreover, temperature controls pores pressure, void ratio and pore water volume forming hysteresis effect (Richard and Mitchell, 1968). So, it is necessary to define a temperature (°C) for quantification shrink – swell phenomenon in soils. It is reported that no single soil property can accurately predict shrink-swell potential (Thomas *et al.*, 2000), perhaps inconsistence results of past studies that remained unclear the role of individual factors. Since, the variation of soil physical and chemical parameters in micro-highs and in micro-lows (Wilding *et al.*, 1990; Bhattacharyya *et al.*, 1999b) thus, it is need to find out the key soil factors responsible for soil shrink – swell. In view of this background, the present study has been undertaken to find out a logical and acceptable method using three different temperatures (25°C- RT, 40°C and 110°C) and devices (COLE box, Cylindrical and MM box) for measuring shrink – swell properties of soils and to relate these values with carbon content and other soil properties.

Materials and Methods

Description of study area

The study area falls under tropical dry sub-humid climate of Maharashtra, India (Fig. 1). All the soils are developed from basaltic alluvium. Other geographic details as given below,

Pedon 1 (P_1) is located at 20°53'3.2"N and 78°41'48.5"E in Seloo village (Seloo series) of Wardha district. The Seloo soils show typical shrink-swell properties (very fine, smectitic, hyperthermic *Typic Haplusterts*) and well drained soils occurring in with 3 to 8 percent slope at an elevation of 270-280 m above MSL. The mean annual temperature of 33.5°C and mean annual rainfall of 993.9 mm. Soils are used for growing banana, vegetables, pulses, cereals and natural vegetation are babul (*Acacia spp.*), neem

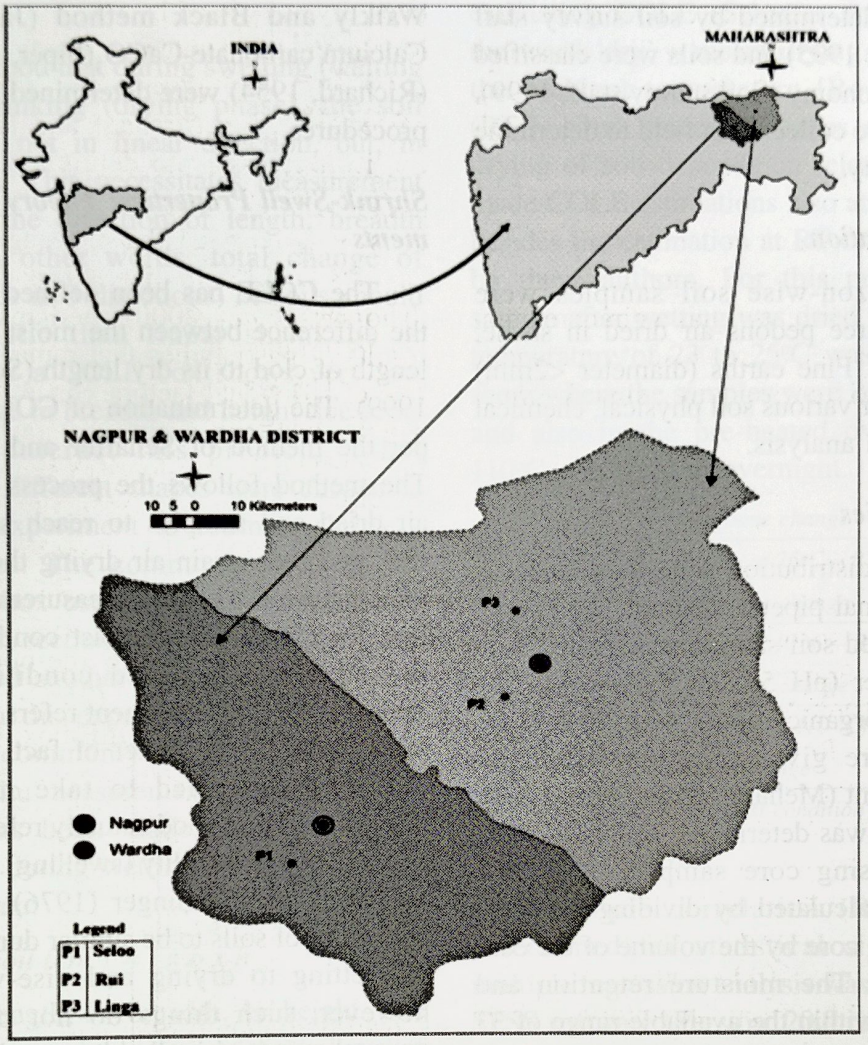

Fig. 1. *Map showing location of Vertisol study sites in Maharashtra*

(*Azadirachta indica),* teak (*Tectona grandis*).

Pedon 2 (P_2) positioned at 21°1'17" North lattitude and 79°4'29"East logitude in Rui village (Rui series) of Nagpur district. Rui soils are classified as fine, smectitic, hyperthermic *Typic Haplusterts* and well drained soils with 1-3% slope at an elevation of 300 m above MSL. The mean annual temperature of 26.8°C and mean annual rainfall of 1127.3 mm. Cropping systems are cotton (*Gossypium sp.*) + Pigeonpea (*Cajanuscajan*) intercropping systems. Natural vegetation for babul, mango (*Magnifera indica),* dub, andkans.

Pedon 3 (P_3) located between 21°14'49"N and 78°37'11"E in Linga village (Linga series) of Nagpur district. Linga soils werefine, smectitic, hyperthermic *Typic Haplusterts* and moderately drained with 0 to 1% slope at an elevation of 420 m above MSL. The mean annual temperature of the area is 25.9°C and mean annual rainfall of 1010.70 mm. Soils are cultivated for Soybean (*Glycine max*), wheat (*Triticum aestivum*), and citrus. Natural vegetation used for babul, and ber (*Zizyphus jujube*).

Field and Laboratory Methods

Total three soil profiles were cut and horizon wise samples collected. Soil morphological

properties were determined by soil survey staff (Soil survey staff, 1995) and soils were classified following soil taxonomy (Soil survey staff, 1999). Core samples were collected in field to determine *in-situ* bulk density.

Soils characterization

Sixteen horizon-wise soil samples were collected from three pedons air dried in shade, crush and sieved. Fine earths (diameter <2mm) soils were used for various soil physical, chemical and mineralogical analysis.

Physical Properties

Particle size distribution was determined as per the international pipette method. The known amount of air-dried soil sample was treated with 1N NaOAc buffer (pH 5.0) to remove $CaCO_3$. After oxidizing organic matter with 30% H_2O_2, the samples were given citrate-bicarbonate-dithionite treatment (Mehara and Jackson, 1960). The bulk density was determined by *in-situ* field moist method using core samples of known volume. It was calculated by dividing the oven dry weight of soil core by the volume of the core (Richard, 1954). The moisture retention and release behavior within the available range of 33 kPa to 1500 kPa were measured on <2 mm soil sample using pressure plate membrane apparatus (Richard, 1954). Available water content (AWC) was determined by using the formula suggested (Gardner *et al.,* 1984) and later modified (Coughlam *et al.,* 1986). The hydraulic conductivity of soils was determined by (Darcy's law) constant head method (Richard, 1954).

Chemical Properties

Soil pH was measured potentiometrically in a soil suspension (1:2.5 soil:water, v/v) (Jackson, 1973). The clear supernatant extract obtained from the suspension used for pH (soil:water, 1:2.5) was utilized for Electrical conductivity (EC) measurement by conductivity bridge (Richard, 1954). Soil Organic Carbon – modified Walkly and Black method (Jackson, 1973), Calcium carbonate-$CaCO_3$(Piper, 1950),soil CEC (Richard, 1954) were determined by the standard procedures.

Shrink-Swell Properties: Theory and Measurements

The COLE has been defined as the ratio of the difference between the moist length and dry length of clod to its dry length (Soil survey staff, 1999). The determination of COLE was done as per the method of Schaffer and Singer (1976). The method follows the process of wetting the air dried soil samples to reach saturation point (SP) and then again air drying the soils at room temperature (RT). Two measurements are taken, first for the length at moist condition (SP, Lm) the other at air- dried condition (RT, Ld). Although, the measurement refers to extensibility (COLE) but, as a matter of fact the moist soils are gradually dried to take measurements. Therefore, the method actually refers to shrinkage rather than extensibility (swelling). It seems likely that Schaffer and Singer (1976) considered the behaviour of soils to be similar during the process of wetting to drying and vise-versa. In soils however, such things do not occur and this unusual process is called hysteresis (Baver *et al.,* 1978). It seem that water content in a soil varies during two different phases such as wetting (wetting air dried soil) and drying (drying a wet soil) under a particular matric potential. There should be therefore, two types of coefficients namely coefficient of linear extensibility (COLE), and coefficient of linear shrinkage (COLS) depicting two different types of measuring shrink – swell characteristics of soils. The following two equations to calculate these two parameters have been developed.

$$COLE = \frac{Lm-Ld}{Ld} \quad \text{.. (i)}$$

$$COLS = \frac{Lm-Ld}{Lm} \quad \text{.. (ii)}$$

where, Lm= Length of moist soil, Ld=Length

of dry soil

It is understood that during swelling (wetting phase) and shrinking (drying phase), the soil manifests itself not in linear direction, but, in three directions. This necessitates measurement of changes in the direction of length, breadth and height. In other words, total change of volume (changes in 3 directions) of soils should be more realistic than linear shrinkage or swelling. Ideally a COLE box shows very low degree of change in breadth and height due to its shape. To counteract this problem, other instruments of different shapes were chosen to carry out the experiment to estimate shrink – swell properties. The commonly used micro-morphological box used to collect soil samples to carry out thin section study of soils was used. Besides we used another type of structure (core box) to carry out this experiment. This cylindrical instrument is commonly used to collect soil sample for in situ measurement for bulk density. An attempt has been made to calculate the volume of soil during wetting and drying phase using the formula:

$$Volume\ of\ soil\ (cm^3) = l \times b \times h \quad .. \text{(iii)}$$

where, l= length, b= breadth, h= height. The formula (iii) was used to calculate the volume of soil in COLE box as well as in micro-morphological box.

For the calculation of volume in the core sampler the following formula (iv) was used.

$$Volume\ of\ core\ (cm^3) = \pi r^2 \times h1 \quad .. \text{(iv)}$$

where, r = radius of circular surface (cm), and h1 = height of the core sample (cm)

The change in volume of soil was calculated by the difference in volume at moist condition. The volume change thus obtained was expressed as percent volume change (PVC). As discussed earlier, keeping in view the hysteresis effect, the PVC was calculated as PVCsw (swelling) and PVCs (shrinkage) by following the equations v, vi, vii, viii. While defining methodology for estimating COLE (Schaffer and Singer, 1976), the word 'dry' – meant drying at atmosphere in the ambient temperature [Room Temperature (RT)]. Now, since RT varies and the effective drying of soil depends on relative humidity, we made COLE estimations also at 40°C and 110°C, besides the estimation at RT originally proposed by these authors. For this purpose the same sample after wetting was dried in RT (a constant temperature of 23 to 25°C was maintained in a room where the samples were kept for air drying) and also in the pre-heated oven to 40°C and 110°C, respectively overnight.

$$PVCsw\ 25°C = \frac{Volume\ change}{(Volume\ at\ 25°C - RT)} \times 100 \quad .. \text{(v)}$$

$$PVCsw\ 40°C = \frac{Volume\ change}{(Volume\ at\ 40\ °C - RT)} \times 100 \quad .. \text{(vi)}$$

$$PVCsw\ 110°C = \frac{Volume\ change}{(Volume\ at\ 110\ °C)} \times 100 \quad .. \text{(vii)}$$

$$PVCs = \frac{Volume\ change}{(Volume\ at\ moist\ condition)} \times 100 \quad .. \text{(viii)}$$

Statistical Analysis

A simple correlation (R^2) values were determined for statistical significance. The multiple regression analysis was carried out using SPSS software (Version. 20.0 released 2011 IBM Corp).

Results and Discussion

Morphological properties

The field morphology of these soils reflects similar geologic parent materials in the eastern part of Maharashtra. Colour of all three pedons were very dark grayish brown is in hue of 10 YR, value 3 to 4 and chroma 2 to 4 in surface and sub-surface horizons (Table 1). Medium to moderate subangular blocky structure was observed with coarse strong angular blocky structure was seen in Bss2, Bss3 in Linga soils. The slickensides were formed at a depth of about 50 cm from surface and extended up to deeper

Table 1. *Field morphological properties of the pedons examined in this study*

Horizon	Depth (cm)	Boundary		Matrix colour (Munsell)	Texture	Coarse fragments (%)	Structure			Consistence			Roots		Efferves cence	Other features	Cracks
		D[a]	T				S	G	Ty	D[b]	M	W	S	Q			
(P1): Wardha District – Seloo Series																	
Ap	0-13			10YR 3/2	C	5-10	m	2	sbk	sh	Vfr	sp	vfm	fc	e	—	
Bw1	13-32			10YR 3/2	C	<5	m	2	sbk	sh	Vfr	sp	vfm	fc	e	—	
Bw2	32-59	c	s	10YR 3/2	C	<5	m	2	abk	sh	F	vsps	f	c	e	PF	
Bss1	59-81	c	s	10YR 3/2	C	<5	m	2	abk	sh	F	vsps	f	F	e	SS	
Bss2	81-115	g	s	10YR 3/2	C	<5	m	2	abk	sh	F	vsps	f	F	e	SS	
BCk	115-145			10YR 3/4	C	25-30	m	2	abk	h	Fr	vsps	f	F	e	—	
(P2): Nagpur District – Rui Series																	
Ap	0-17			10YR 4/2	C	14	m	2	sbk	Sh	Fr	sp	vf	fc	—	—	
Bwk	17-47	c	w	10YR 3.5/2	C	14.5	m	3	sbk	—	Fr	sp	vf	fc	—	PS	
Bssk	47-80	a	s	10YR 3.5/2	C	10.6	m	3	abk	—	Fr	sp	vf	fc	—	SS	
Ck	80-94	Weathered basalt (calcareous)			es	—											
R	94+	Basalt rock															
(P3) : Katol, Nagpur District – Linga Series																	
Ap	0-13			10YR 3/2	C	3.5	m	2	sbk	Sh	Fr	sp	vf	mf	e	—	0.5 cm
Bw	13-33	g	s	10YR 3/2	C	—	m	3	sbk	—	Fr	sp	v	mf	e	PF	
Bw1	33-55	g	s	10YR 3/2	C	—	m	3	sbk,abk	—	Fr	sp	—	F	e	SS	
Bss1	55-81	g	s	10YR 3/2	C	2.3	m	3	abk	—	Fr	sp	—	F	e	SS	
Bss2	81-119	c	s	10YR 3/1.5	C	2.3	c	3	abk	—	Fr	vs,sp	—	F	e	SS	
Bss3	119-150+			10YR 4/2.5	C	2.3	c	3	abk	—	Fr	vs,vp	—	—	e	SS	

PF:Pressure faces; SS: Slickensides, [a]D:Distinctness, T:Topography, cs: Clear smooth, gs: Gradual smooth; c: Clay, S: Size; G: Grade; Ty: Type; m^{2}sbk: medium moderate subangular blocky; m2abk: medium moderate angular blocky; [b]D: dry; M: moist; W: wet; Sh:Slightly hard; h: Hard; vfr: Very friable; fi: Firm; Q: Quantity; vfm: Many very fine; f:Few; fc: Fine common; mf: many few; e: slight effervescence.

layer and characterized by moderate medium to strong coarse angular blocky structure. These soils have hard to hard (dry), friable to firm (moist) and have sticky and plastic to very plastic and very plastic consistence (Table 1). All soils showed slight to strong effervescence with 10% HCl. Horizon boundaries were clear smooth to gradually smooth.

Physical and chemical properties

The clay content of all these alkaline soils was > 50%, except the calcareous horizons (Tables 2 and 3). Bulk density (Mg m^{-3}) of the surface (Ap) layer varied from 1.5 to 1.73 and showing a decreasing trend with soil depth. The available water content (AWC) varied from 9.0to 25.9 percent at surface layers and showing an increasing trend with depths in all soils. Low EC values indicated that these soils were not saline. In all three pedons Ca^{2+} is the dominant exchangeable cations observed, followed that Mg^{2+}, Na^{+} and K^{+} in all depths. The soil organic carbon (SOC) concentrations were observed decreasing with depths and varied 0.6 – 1.0 percent at surface layers of the soils. While, soil inorganic carbon (SIC)was (calculated 12% carbon content in $CaCO_3$) varied from 0.4 -0.9 percent (Table 3). The CEC (cmol (p^{+}) kg^{-1}) of soils varied in range of 49.8 - 69.6, 44.2 - 54.7, and 51.7 - 57.7 for P_1, P_2, and P_3, respectively. The clay CEC value indicates the dominance of smectite (Bhattacharyya *et al.,* 1997; Shirsath *et al.,* 2000). Base saturation percentage exceeding 100 percent (Table 3) indicates the presence of zeolites in soils (Bhattacharyya *et al.,* 1993; 1999a; 2015; Pal *et al.,* 2006). The X-ray diffraction analysis confirms the dominance of smectite and presence of zeolites in these black soils (Thakur, 2007).

Shrink – swell properties

There were four types of shrink-swell parameters determined namely COLE, COLS, PVCsw, and PVCs (Table 4). As the COLE value

Table 2. *Physical properties of the pedons examined in this study soils*

Horizon	Depth (cm)	Particle size distribution (%)			Bulk density (Mg m^{-3})	Water Retention (%)		AWC (%)	HC (cm hr^{-1})
		Sand (200-50µm)	Silt (50-2 µm)	Total Clay (<0.2 µm)		33 kPa	1500 kPa		
(P1): Wardha District – Seloo Series									
Ap	0-13	1.0	34.0	65.0	1.7	44.8	19.2	25.6	0.5
Bw1	13-32	1.0	34.0	65.0	1.9	43.2	16.8	26.4	0.5
Bw2	32-59	2.0	33.0	65.0	1.8	51.3	22.5	28.8	0.8
Bss1	59-81	1.0	30.0	69.0	1.8	54.1	22.6	31.5	0.5
Bss2	81-115	1.0	30.0	69.0	1.7	55.1	22.0	33.1	0.5
BCk	115-145	25.0	45.0	30.0	1.7	48.0	20.4	27.6	0.7
(P2) : Nagpur District – Rui Series									
Ap	0-17	0.9	34.7	64.4	1.5	37.8	28.8	9.0	0.2
Bwk	17-47	1.1	31.4	67.5	1.6	34.2	21.6	12.6	0.3
Bssk	47-80	0.8	30.9	68.3	1.5	41.3	25.9	15.4	0.6
Ck	80-94	3.2	25.8	71.0	1.5	–	31.0	12.8	–
(P3) : Katol, Nagpur District – Linga Series									
Ap	0-13	0.8	35.1	64.1	1.5	42.0	22.4	19.6	5.0
Bw	13-33	0.5	33.5	66.0	1.5	41.1	22.1	19.0	2.7
Bw1	33-55	0.5	33.5	66.0	1.5	44.3	21.4	22.9	1.2
Bss1	55-81	0.3	29.5	70.2	1.5	45.3	22.4	22.9	1.6
Bss2	81-119	0.3	30.1	69.6	1.4	47.6	23.9	23.7	1.4
Bss3	119-150+	0.2	28.4	71.4	1.5	42.7	24.8	22.9	1.6

Table 3. *Chemical properties of the pedons examined in this study*

Horizon	Depth (cm)	pH (1:2.5) water	EC (dS m^{-1})	SOC (%)	SIC (%)	$CaCO_3$ (%)	Exchangeable Cationsc mol (p+)kg^{-1}					BS (%)	CEC c mol (p+) kg^{-1}	ESP (%)
							Ca2+	Mg2+	Na+	K+	Sum			
(P1): Wardha District – Seloo Series														
Ap	0-13	8.9	0.19	0.92	0.4	3.3	53.4	7.6	0.2	1.5	62.4	90	69.6 (104)[a]	0.2
Bw1	13-32	8.2	0.14	0.73	0.4	3.6	53.9	10.1	0.2	0.9	64.3	113	57.0 (88)	0.3
Bw2	32-59	8.1	0.13	0.53	0.4	3.1	57.9	12.0	0.2	0.6	70.8	123	57.4 (88)	0.4
Bss1	59-81	8.0	0.14	0.47	0.4	2.8	56.7	16.2	0.2	0.7	73.4	127	57.9 (84)	0.3
Bss2	81-115	8.0	0.16	0.46	0.4	3.2	58.2	14.6	0.2	0.6	73.6	129	56.9 (82)	0.4
BCk	115-145	8.2	0.16	0.24	0.4	3.7	51.5	15.5	0.2	0.3	67.3	135	49.8 (166)	0.5
(P2) : Nagpur District – Rui Series														
Ap	0-17	8.0	0.20	0.60	0.6	5.0	42.0	7.4	1.6	1.3	52.3	118	44.2 (106)	3.0
Bwk	17-47	7.9	0.21	0.50	0.4	4.0	43.4	6.0	1.5	0.9	51.8	94	54.7 (107)	3.0
Bssk	47-80	8.0	0.20	0.40	0.7	6.0	40.8	3.6	1.5	0.9	46.8	89	52.4 (103)	3.0
Ck	80-94	7.9	0.20	0.30	0.9	8.0	40.8	4.6	1.5	0.9	47.8	87	54.6 (77)	3.0
(P3) : Katol, Nagpur District – Linga Series														
Ap	0-13	7.7	0.16	1.0	0.7	6.0	40.4	10.8	0.3	0.5	52.0	90	57.7 (90)	0.5
Bw	13-33	7.9	0.17	0.7	0.7	6.4	40.7	6.4	0.3	0.6	48.0	85	56.4 (85)	0.5
Bw1	33-55	7.8	0.17	0.6	0.6	5.1	40.7	8.2	0.3	0.6	49.8	88	56.6 (86)	0.5
Bss1	55-81	7.9	0.15	0.5	0.8	6.7	40.9	11.0	0.3	0.6	52.8	94	56.4 (80)	0.5
Bss2	81-119	7.8	0.15	0.4	0.5	4.6	38.6	13.4	0.3	1.0	53.3	95	56.0 (80)	0.5
Bss3	119-150+	7.8	0.05	0.3	0.7	6.2	37.8	17.3	0.3	0.7	56.1	109	51.7 (70)	0.6

[a]Parentheses shows clay CEC values

of all the pedons were exceeding 10 and volume change were >30 the categories of swell (COLE) – shrink (volume change) and their ratings were severe (Schaffer and Singer, 1976). In general COLE is found to be more than COLS at any temperatures of measurement (Table 4). These values were used to calculate percent change over the values obtained at room temperature (RT). A closer view of dataset (Table 4) shows 0 to 136 percent increase of COLE value at 40°C over RT. The corresponding values for 110°C are 4 to 191 whereas, the percent change value of COLS vary from 0 to 120 at 40°C and 0 to 140 at 110°C over RT. It is encouraging to see the data presented in Table 4 that the changes of COLE and COLS values indicate a very high degree of variation between RT and 40°C values. However, both COLE and COLS are almost similar at 40°C and at 110°C. When both COLE and COLS values were used to calculate percent change over RT and 40°C at 40°C, and 110°C, respectively, it showed relatively less degree of change in (Fig. 2a, b). The soil volume change (Table 4) wasnot steadied at 40°C as like the shrink –swell in linear direction (COLE and COLS). As a matter of fact, volume of soils at 110°C was found to be changed to 9-113 percent over

the change noticed at 40°C (Fig.2c). The corresponding values for PVCs were in the range from 3-61 percent (Fig.2d). From the above discussion, it can be inferred that, heating the soil cake for linear measurement to 110°C does not bring any high degree of change. This is shown through the COLE and COLS values which were nearly stabilized at 40°C; therefore, we recommend that these values should be measured and to be reported at 40°C instead of room temperature as is commonly practiced (RT). Besides, high degree of variation found in the percent volume change (PVC) data over 40°C at 110°C, hence, the shrink – swell properties should be expressed in terms of volume change at 110°C. Thus, developed equations 'ii'and 'viii' for linear and volume change measurement, respectively should follow for determination shrink-swell in black soils.

Shrink –swell properties measured using different methods

It has been discussed earlier that shrink – swell properties measured by three different types

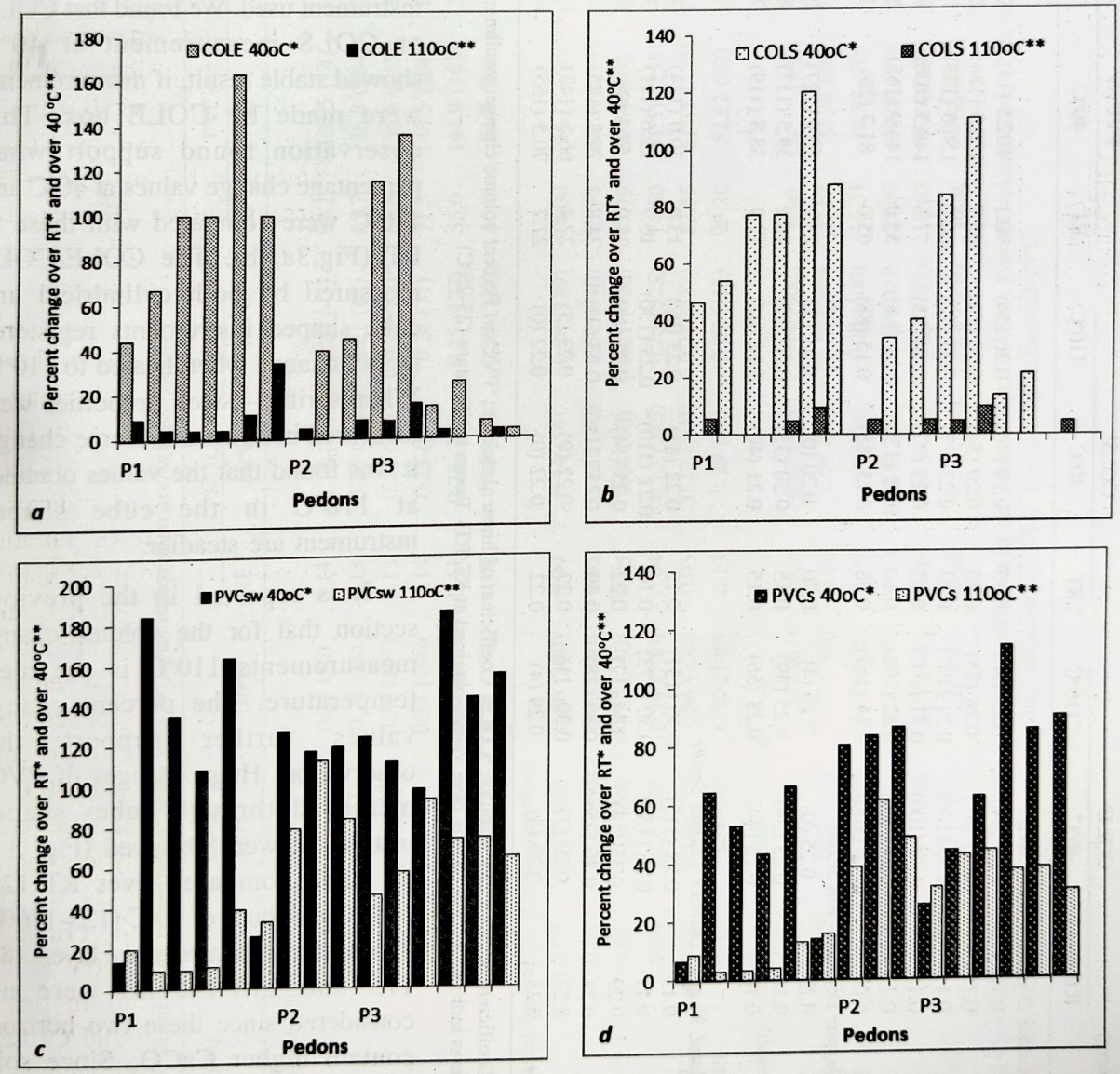

Fig. 2. *Percent change over RT at 40°C* and over 40°C at 110°C** for COLE (a), and CLOS (b), PVCsw (c), and for PVCs (d)*

Table 4. *Shrink-swell properties of the pedons examined in this study*

Depth (cm)	COLE[a]		COLS[b]		PVCsw[c]		PVCs[d]		
	RT[f]	40°C	110°C	RT	40°C	110°C	RT	40°C	110°C	RT	40°C	110°C
(P1): Wardha District – Seloo Series												
0-13	0.16	0.23 (44)[e]	0.25 (56)	0.13	0.19 (46)	0.20 (54)	90.1	102.5 (14)	123.0 (37)	47.4	50.6 (7)	55.1 (16)
13-32	0.15	0.25 (67)	0.26 (73)	0.13	0.20 (54)	0.20 (54)	65.7	186.8 (184)	203.5 (210)	39.6	65.1 (64)	67.0 (69)
32-59	0.15	0.30 (100)	0.31 (107)	0.13	0.23 (77)	0.23 (77)	66.6	156.6 (135)	171.2 (157)	39.9	61.0 (53)	63.1 (58)
59-81	0.15	0.30 (100)	0.31 (107)	0.13	0.23 (77)	0.24 (85)	71.3	148.5 (108)	164.5 (131)	41.6	59.7 (44)	62.1 (49)
81-115	0.11	0.29 (164)	0.32 (191)	0.10	0.22 (120)	0.24 (140)	55.0	144.9 (163)	201.7 (267)	35.5	59.1 (66)	66.8 (88)
115-145	0.09	0.18 (100)	0.24 (167)	0.08	0.15 (88)	0.15 (88)	65.0	81.7 (26)	108.5 (67)	39.3	44.9 (14)	52.0 (32)
(P2) : Nagpur District – Rui Series												
0-17	0.25	0.25 (0)	0.26 (4)	0.20	0.20 (0)	0.21 (5)	25.1	56.9 (127)	101.8 (306)	20.1	36.3 (81)	50.4 (151)
17-47	0.18	0.25 (39)	0.25 (39)	0.15	0.20 (33)	0.20 (33)	18.2	39.5 (117)	84.0 (362)	15.4	28.3 (84)	45.7 (197)
47-80	0.18	0.26 (44)	0.28 (56)	0.15	0.21 (40)	0.22 (47)	17.7	38.8 (119)	71.3 (303)	15.0	28.0 (87)	41.6 (177)
80-94	–	–	–	–	–	–	–	–	–	–	–	–
(P3) : Katol, Nagpur District – Linga Series												
0-13	0.13	0.28 (115)	0.30 (131)	0.12	0.22 (83)	0.23 (92)	13.4	30.0 (124)	43.7 (226)	18.4	23.1 (26)	30.4 (65)
13-33	0.11	0.26 (136)	0.30 (173)	0.10	0.21 (110)	0.23 (130)	10.7	22.6 (111)	35.5 (232)	19.7	28.4 (44)	40.5 (106)
33-55	0.29	0.33 (14)	0.34 (17)	0.22	0.25 (14)	0.25 (14)	28.9	57.3 (98)	110.4 (282)	22.4	36.4 (63)	52.5 (134)
55-81	0.24	0.30 (25)	0.30 (25)	0.19	0.23 (21)	0.23 (21)	24.8	70.8 (185)	122.7 (395)	19.3	41.4 (115)	56.8 (194)
81-119	0.27	0.29 (7)	0.30 (11)	0.22	0.22 (0)	0.23 (5)	27.4	66.5 (143)	115.7 (322)	21.5	39.9 (86)	55.1 (156)
119-150+	0.28	0.29 (4)	0.29 (4)	0.22	0.22 (0)	0.22 (0)	27.7	70.5 (155)	115.9 (318)	21.7	41.3 (90)	53.7 (147)

[a]COLE:Coefficient of linear extensibility; [b]COLS: Coefficient of linear shrinkage; [c]PVCsw: Percent volume change, swelling; [d]PVCs: Percent volume change, shrinkage;
[e]Parentheses indicate percent change over values obtained at RT.[f]RT: Room temperature (23-25°C)

of instruments *viz;* COLE box, core, and micromorphology box at RT, 40°C and 110°C. Only the Seloo soils (P_1) were analyzed with the three types of instruments (Table 5). It was observed that COLE and COLS measured by core or cube shaped instruments were found less than COLE box. The data generated (Table 5) clearly showed that COLE and COLS measured at 110°C were nearly similar irrespective of type of instrument used. We found that COLE or COLS measurement at 40°C showed stable result, if measurements were made by COLE box. This observation found support when percentage change values at 40°C and 110°C were compared with those in RT (Fig.3a, b). The COLE/COLS measured by both cylindrical and cube shaped instruments registered higher change when heated to 110°C. When shrink – swell properties were measured in terms of volume change, it was found that the values obtained at 110°C in the cube shaped instrument are steadier.

It is reported in the previous section that for the volume change measurements 110°C is the ideal temperature. The percent change values further support this observation. Huge changes of PVCs measured through cube- shaped instrument were observed (Fig. 3 c, d) when compared over RT (22-145%) and those of 40°C (123-176%). The data of two subsurface layers (81-115 and 115-145cm) were not considered since these two horizons contain higher $CaCO_3$. Since soils shrink and swell in all directions in the field condition, it seems

Table 5. *Shrink-swell properties of Seloo soils (P_1) with different measuring instrument*

Depth (cm)	COLE[a]			COLS[b]			PVCsw[c]			PVCs[d]		
	RT[f]	40°C	110°C	RT	40°C	110°C	RT	40°C	110°C	RT	40°C	110°C
Rectangular (Normal COLE box)												
0-13	0.16	0.24 (50)[e]	0.25 (56)	0.14	0.19 (36)	0.20 (43)	90.1	102.5 (14)	123.0 (37)	47.4	50.6 (7)	55.1 (16)
13-32	0.15	0.26 (73)	0.26 (73)	0.13	0.20 (54)	0.21 (62)	65.7	186.8 (184)	203.5 (210)	39.6	65.1 (64)	67.0 (69)
32-59	0.15	0.31 (107)	0.31 (107)	0.13	0.23 (77)	0.24 (85)	66.6	156.6 (135)	171.2 (157)	39.9	61.0 (53)	63.1 (58)
59-81	0.16	0.30 (88)	0.33 (106)	0.14	0.23 (64)	0.24 (71)	71.3	148.5 (108)	164.5 (131)	41.6	59.7 (44)	62.1 (49)
81-115	0.12	0.29 (142)	0.32 (167)	0.11	0.23 (109)	0.25 (127)	55.0	144.9 (163)	201.7 (267)	35.5	59.1 (66)	66.8 (88)
115-145	0.09	0.18 (100)	0.24 (167)	0.09	0.15 (67)	0.19 (111)	65.0	81.7 (26)	108.5 (67)	39.3	44.9 (14)	52.0 (32)
Cylindrical instrument (CORE sampler)												
0-13	0.09	0.17 (89)	0.36 (300)	0.09	0.14 (56)	0.26 (189)	18.00	24.11 (34)	71.14 (295)	15.00	19.42 (29)	41.90 (179)
13-32	0.05	0.13 (160)	0.47 (840)	0.05	0.12 (140)	0.37 (640)	13.98	52.24 (274)	125.90 (801)	12.27	34.31 (180)	51.69 (321)
32-59	0.06	0.09 (50)	0.27 (350)	0.05	0.08 (60)	0.21 (320)	17.79	59.59 (235)	131.46 (639)	15.10	37.34 (147)	56.79 (276)
59-81	0.04	0.15 (275)	0.34 (750)	0.04	0.13 (225)	0.25 (525)	14.50	51.51 (255)	120.59 (732)	12.66	33.99 (168)	54.66 (332)
81-115	0.04	0.14 (250)	0.34 (750)	0.03	0.12 (300)	0.25 (733)	22.55	61.35 (172)	130.22 (477)	18.40	38.02 (107)	56.56 (207)
115-145	0.15	0.24 (60)	0.39 (160)	0.13	0.19 (46)	0.28 (115)	29.20	52.62 (80)	174.2 (497)	22.60	34.47 (53)	63.53 (181)
Cube-shaped instrument (Micromorphology box)												
0-13	0.03	0.08(167)	0.23 (667)	0.03	0.07 (133)	0.18 (500)	8.60	24.11 (180)	78.83 (817)	7.92	19.42 (145)	44.08 (457)
13-32	0.05	0.07 (40)	0.23 (360)	0.05	0.06 (20)	0.19 (280)	22.81	33.38 (46)	125.90 (452)	18.57	25.03 (35)	55.73 (200)
32-59	0.04	0.06 (50)	0.25 (525)	0.04	0.05 (25)	0.20 (400)	15.31	22.89 (50)	105.94 (592)	13.27	18.63 (40)	51.44 (288)
59-81	0.12	0.13 (8)	0.30 (150)	0.10	0.11 (10)	0.23 (130)	23.03	29.69 (29)	110.28 (379)	18.72	22.89 (22)	52.44 (180)
81-115	0.10	0.13 (30)	0.27 (170)	0.09	0.11 (22)	0.21 (133)	18.93	54.74 (189)	114.07 (503)	13.92	35.37 (154)	53.28 (283)
115-145	0.04	0.11 (175)	0.20 (400)	0.04	0.10 (150)	0.28 (600)	10.86	64.56 (494)	96.19 (786)	9.80	39.23 (300)	49.03 (400)

[a]COLE:Coefficient of linear extensibility; [b]COLS: Coefficient of linear shrinkage; [c]PVCsw: Percent volume change, swelling; [d]PVCs: Percent volume change, shrinkage;
[e]Parentheses indicate percent change over values obtained at RT.[f]RT: Room temperature (23-25°C)

appropriate that a cube shaped instrument should provide suitable space in x, y, z directions for uniform shrinkage and swelling. Therefore, it can be concluded that the micro morphological box should be an ideal instrument to measure volume change in soils.

Relation between shrink – swell parameters and soil properties

An effort was made to develop an ideal shrink-swell measurement technique, and to develop relationship between the four mechanical properties (COLE, COLS, PVCsw, and PVCs) and the physical and chemical properties of soils. It has also been shown that out of three different temperatures COLS at 40°C and PVCs at 110°C were ideal. In respect of instrument the cube shaped (micromorphology box) was the best option than COLE box and core (cylindrical shape) for measuring shrink–swell potential. Only Seloo soils (P_1) were used to measure PVC by micromorphology box. Using PVCs values measured by micromorphology box the following relation was developed with COLE box.

PVCs 110°C MM box = 0.8 (PVCs 110°C COLE box).....(ix)

The PVCs of Rui (P_2) and Linga (P_3) soils

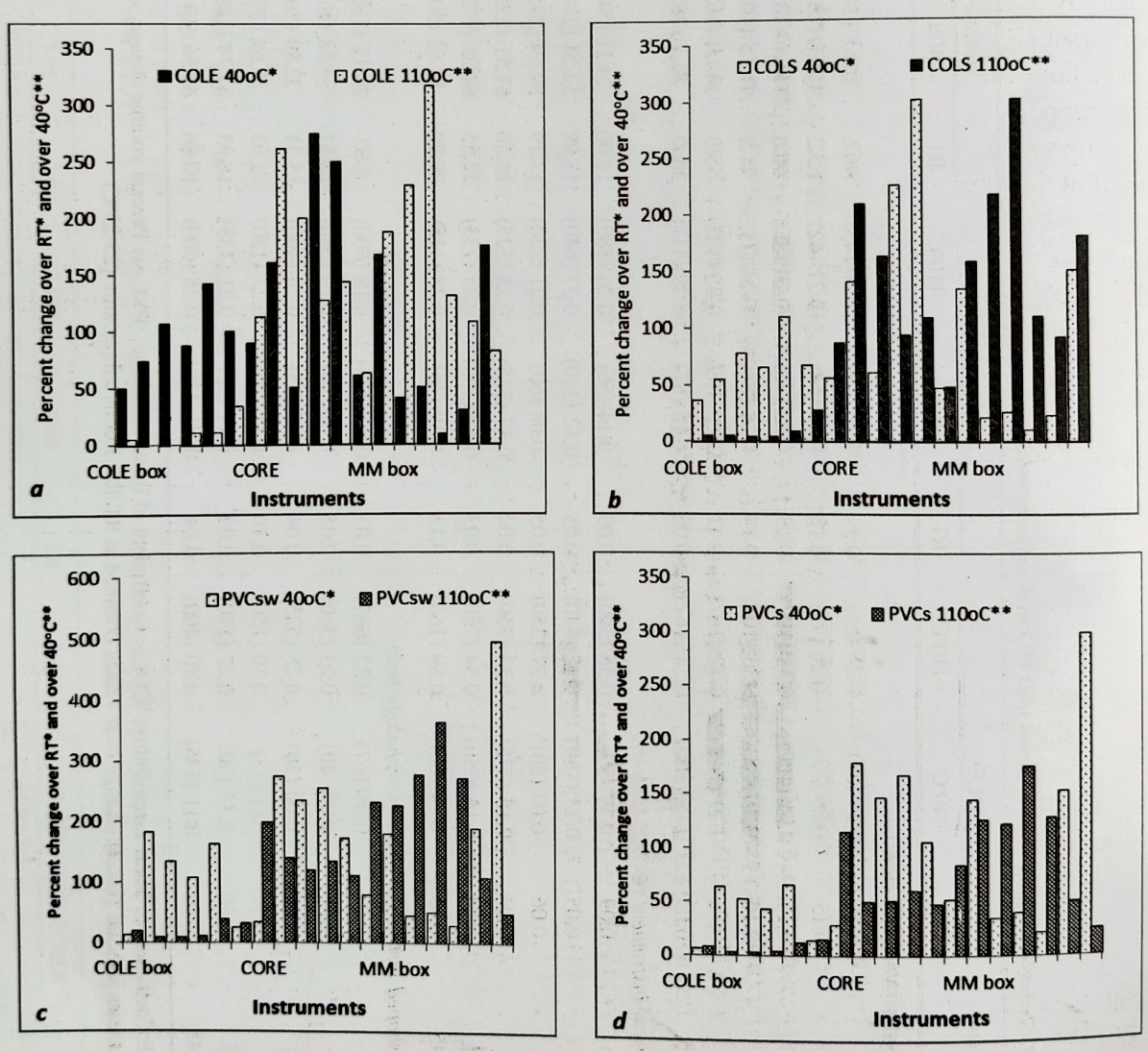

Fig. 3. *Percent change over RT at 40°C* and over 40°C at 110°C** for COLE (a), COLS (b), PVCsw (c), PVCs (d) in different measuring instrument*

measured by COLE box were converted to PVCs 110°C values for MM box and these values were used to find out relation with soil properties. The shrink-swell parameters were always kept as independent variable while other parameters were used as dependent variables (Table 6). The shrink-swell behaviour of soils varied as functions of soil properties, climate, vegetation, and management practices. Here only soil properties are being discussed. Smectite is monotonously presented in the studied soils and therefore, were excluded from other soil parameters. Carbon content in soils consists of SOC and SIC. Small changes of both SOC and SIC content significantly affects soil properties. From the larger dataset (Bhattacharyya *et al.,* 2009) it was described how the soil bulk density (BD) as a physical property influenced both SOC and SIC accumulation in soils with more (> 900mm) and less rainfall (<900mm) eco-regions. It is well known that SOM in soils improves pores and structure, thus soils could hold more waterand could shrink more upon drying. This was illustrated when the study of drying and wetting cycles on Histosols and Gleysols in Germany, reported that organic-rich soil shrink more and swells less than inorganic soils (Peng *et al.,* 2007). It has also been reported that no quantitative information is available relating soil physical properties and SOC (Bovin *et al.,* 2009), particularly for shrink–swell phenomena. The present study however did not show any significant relationship in cases of COLS 40°C (R^2 = 0.013, r = 115) and PVCs 110°C (R^2 = 0.105, r = - 324) with SOC (Smith *et al.,* 1985; Gray and Allbrook, 2002). On the contrary, it was reported that positive correlation existed between SOC and shrinkage in both surface and sub-surface soils (Reeve *et al.,* 1980). It has also been mentioned that removal of SOM increases swelling capacity of soils due to the adsorption of SOM on clay sites (Franzmeier and Ross, 1968). Contrary to this shrinkage of soils increases with increasing SOC content in the smectitic clay soils (Bovine *et al.,* 2009). It seems, therefore, that establishing soil shrink – swell relationship with SOC is not an easy task. However, in this study the negative correlation between SOC and PVCs 110°C appears more logical. The $CaCO_3$ (SIC) dominantly present as

Table 6. *Relation between COLS 40°C, PVCs110°C and studied soils properties*

Soil parameters	COLS 40°C				PVCs 110°C			
	R^{2a}	r^b	p-value[c]	p-value[d]	R^{2a}	r^b	p-value[c]	p-value[d]
SOC	0.013	0.115	0.342	0.684	0.097	-0.311	0.129	0.259
SIC	0.120	0.346	0.103	0.206	0.331	-0.575	0.12*	0.025*
BD	0.028	-0.167	0.276	0.553	0.459	0.677	0.003**	0.006**
AWC	0.012	0.111	0.347	0.693	0.462	0.679	0.003**	0.005**
TC	0.593	0.770	0.000**	0.001**	0.006	0.080	0.388	0.776
SILT	0.540	-0.735	0.001**	0.002**	0.038	-0.195	0.243	0.487
CEC	0.032	0.180	0.260	0.521	0.028	0.167	0.276	0.553
HC	0.054	0.232	0.203	0.406	0.438	-0.662	0.004**	0.007**
Ca2+	0.034	-0.183	0.257	0.513	0.465	0.682	0.003**	0.005**
Mg2+	0.001	0.027	0.462	0.924	0.234	0.484	0.034*	0.068
Na+	0.025	-0.158	0.287	0.574	0.157	-0.396	0.072	0.144
K+	0.015	-0.123	0.331	0.662	0.006	0.077	0.392	0.785

SOC: Soil organic carbon; SIC: Soil inorganic carbon; BD: Bulk density; AWC: Available water content; TC: Total clay; CEC: Cation exchange capacity; HC: Hydraulic conductivity; Ca^{2+}: Calcium; Mg^{2+}: Magnesium; Na+: Sodium; K^+: Potassium

[a]Regression coefficient; [b]Pearson correlation (r); [c]p-value one tailed; [d]p-value two tailed; *$P \leq 0.05$, **$P \leq 0.01$

lime nodules has been reported to decrease BD in black soils. There was significant relationship found between SIC with PVCs 110°C (R^2= 0.331, r = - 575*) unlike the COLS 40°C (R^2= 0.120, r = 346). Elsewhere, a negative correlation have been reported between carbonate (calcite minerals) content with COLE (Badia *et al.,* 2015) whereas, little shrink-swell potential recorded in presence of high SIC ($CaCO_3$) concentration (>80 g kg^{-1}) in Vertisols (*UdicHaplusterts*) catena of Texas (Dinka, 2011).

Physical condition of soils mainly depends on nature of SOM. Higher the SOM lower the soil bulk density making soils lighter and porous showing low shrink-swell phenomenon. This relation was established when shrink swell properties measured as PVCs 110°C as compared to COLE 40°C (Table 6). Available water content in soils depends on clay content and mineral present in clay. Smectite mineral in black soils hold water to great extent to increase AWC. Higher AWC indicates high clay content and for black soils it indirectly indicates larger proportion of smectite minerals. Since more smectite increases swell shrink behavior of black soils, it was expected a good relationship between AWC and shrink swell parameters. In present study a stronger correlation was observed with PVCs 110°C than COLS 40°C (Table 6). Similar correlation was observed with hydraulic conductivityof soils.

Amount and type of clay influence shrink swell behavior (Franzmeier and Ross, 1968; Smith *et al.,* 1985; Bhattacharyya *et al.,* 1997). High correlation coefficient between COLS 40°C (p<0.001) and PVCs 110°C with total clay (TC) was due to more smectite found in TC (Table 6). Silt fractions also contain smectite but in subordinate quantitymaking an inverse relationship with silt content. Lesser COLE was reported in presence of silt than that of clay in sub Mediterranean climate (Badia *et al.,* 2015). CEC of the soils have been an important soil parameter attributed to high shrink- swell soils (Thomas *et al.,* 2000). In soils it is largely controlled by clay fractions in black soils which are dominated with smectitic minerals. As expected, in the present investigation a positive correlation was found between CEC and COLS (40°C), and PVCs (110°C).

Presence of organic/inorganic colloids in soil is important for soil solutions – matrix interactions. The smectite [(Na, $Ca_{0.5}$) Al_2{(Si, Al)$_4$ O_{10}.nH_2O}] mostly exchanges Ca^{2+}, Mg^{2+} in black soils. On clay site exchangeable cations (Ca^{2+}, Mg^{2+}, Na^+ and K^+) are influences the soil water retention characteristics (Balpande *et al.,* 1996; Satyavati *et al.,* 2014). More calcium ions become better soil structure to increases HC which decreases the swell-shrink process. The present study supports a significant positive relation between Ca^{2+} ions and PVCs 110°C (R^2 = 0.465, r = 0.682**) and a negative relation with COLS 40°C. Sodium has been found to increase pH and dispersion of finer particles. Increase in Na^+ causes soil sodicity (Balpande *et al.,* 1996), and slaking aggregates (Shabtai *et al.,* 2014) that increase shrink- swell properties of black soils. Significant relation were reported between COLE and Na^+ ions in recent past (Anderson *et al.,* 1973; Simon *et al.,* 1987) however, perhaps low concentration of Na+ in studied soils did not bring good relation (Gray and Allbrook, 2002). Mg^{2+} ions are also reported to behave like Na^+ ions, and have greater water retention (Satyavathi *et al.,* 2014), thus, greater hydration radii than Ca^{2+} (Dontsova and Norton, 2002). Mg^{2+} indirectly accumulates Na^+ in soil i.e. Mg^{2+} induces sodicity effects soil hydraulic conductivity (Suguru, 2015). It means, the thickness of stern's layer may be wider for Mg^{2+} than Ca^{2+} and thus, may lead dispersion of finer particles consequently deteriorate the soil structure (Suguru, 2015) and favors shrink-swell process. The Mg^{2+} ions significantly correlated with PVCs 110°C (R^2 = 0.234, r = 0.484*). The data set discussed proved our hypothesis that $CaCO_3$, ESP and EMP are also responsible for

shrink-swell phenomena in Vertisols and associated soils. K^+ ion has little ability to cause swelling (Spark, 2002) could be the reason there was no significant relationship found, but minerals K^+ closely related to clay content in smectite dominate soils (Sharply, 1989). The K^+ ion were positively correlated with PVCs 110°C and negatively with COLS 40°C (Table 6)

Out of total 12 combination of methods *viz.*, COLE (25°C, 40°C, 110°C), COLS (25°C, 40°C, 110°C), PVCsw (25°C, 40°C, 110°C), PVCs (25°C, 40°C, 110°C) to estimate shrink-swell potential, COLS 40°C and PVCs 110°C were found as most promising. It was shown how these two shrink – swell parameters are related with 12 selected soil properties. Since, shrink – swell process is controlled by more than one variables, an effort was made to find out how this process is related with multiple variables. Judging by the R^2 values five parameters were found as acceptable. Accordingly equations were developed for COLS at 40°C and PVCs at 110°C as follows:

COLS 40°C = –0.152 + 0.003 TC + 0.028 BD – 0.028 SOC + 0.043 SIC + 0.003 Silt (R^2 = 0.63; SE = 0.0174).....(x)

PVCs 110°C = –32.42 + 0.426 TC + 30.816 BD –18.098 SOC – 8.385 SIC + 0.353 Silt (R^2 = 0.69; SE = 5.7029) .....(xi)

Results indicate that a regression model of COLS 40°C was positively correlated with TC and BD, SIC and Silt and negatively correlated with SOC (Eq. x). PVCs 110°C, on the other hand, was positively correlated with BD, TC and silt and negatively correlated with SOC and SIC (Eq. xi). The R^2 value in both the occasion (equation 'x' and 'xi') are more than the table value of R^2 (linear correlation coefficient test) and therefore is significant.

Conclusions

Cube-shaped box is the best tool when compared to a rectangular box for the estimation of shrink-swell activity in Vertisols and associated soils. Besides, COLS 40°C (linear measurement) and PVCs 110°C (volume change measurement) are good predictors for quantifying shrink-swell parameters in black soils of India. The information provided is expected to deliver revised knowledge base for research, education, farming, engineering and other uses of shrink – swell soils not only in India but also elsewhere.

Acknowledgment

This study was completed with support from Dr. Panjabrao Deshmukh Krushi Vidyapeeth, Akola and the Director, Head, and staffs of Soil Resources Studies Division, ICAR-National Bureau of Soil Survey and Land Use Planning, Nagpur are gratefully acknowledged. We are very gratified for technical assistance provide by Mr.'s. SL Durge, BM Kamble former-Senior Technical officer, NBSS & LUP at field and laboratory work.

References

Acquaye, D.K., Downone, G.N., Mermut, A.R., Arnuad, R.T. 1992. Micromorphology and minerology of cracking soils from the Accra plains of Ghana. *Soil Sci. Soc. Am. J.* **56** : 193-201.

Anderson, J.U., Fadul, K.E., Oconnor, G.A. 1973. Factors affecting the coefficient of linear extensibility in Vertisols.*Soil Sci. Soc. Am. Proc.* **37**: 296-299.

Badia, D., Diego, O., Doz, J.R., Casanova, J., Poch, R.M. and Gonzalez, M.T.G. 2015. Vertic features in a soil catena developed on eocene marls in the inner depression of the Central Spanish Pyrenees. *Catena.* **129** : 86-94.

Balpande, S.S., Deshpande, S.B., Pal, D.K. 1996. Factor and process of soil degradation in

Vertisols of Purna Valley, Maharashtra, India. *Land Degrad. Dev.* **7**: 313-324.

Baver, L.D., Gardner, W.H. and Gardner, W.R., 1978. Water Retention in Soil Physics, 4th edition, Publication by Wiley Estern Limited, New Delhi.Pp.498.

Bhattacharyya, T., Chandran, P., Ray, S.K., Pal, D.K., Mandal, C. and Mandal, D.K. 2015. Distribution of zeolitic soils in India. *Curr. Sci.* **109 (9)** : 1305-1313.

Bhattacharyya, T., Pal, D.K. and Deshpande, S.B., 1997. On kaolinitic and mixed mineralogy classes of shrink-swell soils. *Aust. J. Soil Res.* **35**: 1245-1252.

Bhattacharyya, T., Pal, D.K. and Despande, S.B., 1993. Genesis and transformation of minerals in the form of red (Alfisols) and black (Inceptisols and Vertisols) soils on Deccan basalt. *J. Soil Sci.* **44** : 159-171.

Bhattacharyya, T., Pal, D.K. and Srivastava, P. 1999a. Role of zeolites in persistence of high altitude ferruginous Alfisols of the Western Ghats, India. *Geoderma.* **90**: 263-276.

Bhattacharyya, T., Pal, D.K. and Velayutham, M., 1999b. A mathematical equation to calculate linear distance of cyclic horizon in dark clays. *Soil Surv. Horiz.* **40** : 127-133.

Bhattacharyya, T., Ray, S.K., Pal, D.K., Chandran, P., Mandal, C. and Wani, S.P. 2009. Soil carbon stocks in India- issues and priorities. *J. Indian Soc. Soil Sci.* **57(4)**: 461-468.

Bhuse, S.R., Vaidya, P.H., Bhattacharyya, T. and Pal, D.K. 2001. An improvised method to determine clay smectite in Vertisols. *Clay Res.* **20:** 65-72.

Boivin, P., Schafer, B. and Sturny, W., 2009. Quantifying the relationship between soil organic carbon and soil physical properties using shrinkage modeling. *Eur. J. Soil Sci.* **60**: 265-275.

Coughlam, K.J., Garry, M.C. and Smith, G.D. 1986. The physical and mechanical characteristics of Vertisols, In: First regional seminar on management of Vertisols under semi-arid conditions, IBSRAM Proc. No. 6, Nairobi, Kenya pp. 89-106.

Davidson, S.E. and Page, J.B., 1956. Factors influencing swelling and shrinkage in soils. *Soil Sci. Soc. Am. Proc.* **20**: 320-324.

Dinka, T.M. 2011. Shrink–swell dynamics of Vertisol catenae under different land uses. PhD Thesis.Texas A&M University, College station, TX Pp. 134.

Dinka, T.M. and Lascano, R.J. 2012. Challenges and limitations in studying the shrink-swell and cracks dynamics of Vertisols soils. *Open J. Soil Sci.* **2** : 82-90.

Dontsova, K.M. and Norton, L.D., 2002. Clay dispersion, infiltration and erosion as influenced by exchangeable Ca and Mg. *Soil Sci.* **167(3)**: 184-193.

Franzmeier, D.P. and Ross, S.J. 1968. Soil swelling: laboratory measurement and relation to other soil properties. *Soil Sci. Soc. Am. Proce.* **32**: 573-577.

Gardner, E.A., Shaw, R.J., Smith, G.D., Coughlan, K.J. 1984. Plant available water capacity concept, measurement, prediction, in: McGarity, J.W., Hoult, E.H., Co, H.B. (Eds.), Properties and Utilization of Cracking Clay Soils. Univ. of New England, Asmidale, pp. 164-175.

Gray, C.W. and Allbrook, R., 2002. Relationships between shrinkage indices and soil properties in some New Zealand soils. *Geoderma.* **108**: 287– 299.

Groenevelt, P.H. and Grant, C.D. 2004. Analysis of soil shrinkage data. *Soil Tillage Res.***79**: 71–77.

Grossman, R.B., Brasher, B.R., Franzmeier, D.P. and Walker, J.L. 1968. Linear extensibility as calculated from natural-clod bulk density

measurements. *Soil Sci. Soc. Am. Proc.* **32**: 570-573.

Igwe, C.A. 2003. Shrink-swell potential of flood-plain soils in Nigeria in relation to moisture content and mineralogy.*Int. Agrophy.* **17**: 47-55.

Jackson, M.L. 1973. Soil Chemical Analysis, Prentice Hall, New Delhi, India pp. 498.

Kadu, P.R., Vaidya, P.H., Balpande, S.S., Satyavathi, P.L.A. and Pal, D.K. 2003. Use of hydraulic conductivity to evaluate the suitability of Vertisols for deep-rooted crops in semi-arid parts of central India. *Soil Use Manage.* **19** : 208-216.

McCormack, D.E. and Wilding, L.P. 1975. Soil properties influencing swelling in Canfield and Geeburg soils. *Soil Sci. Soc. Am. J.* **39**: 496-502.

Mckenzie, N.J., Jacquier, D.J., Ringrose-Voase, A.J. 1994. A rapid method for estimating soil shrinkage. *Aus. J. Soil Res.* **32(5)**: 931 – 938.

Mehara, O.P. and Jackson, M.L., 1960. Iron oxide removal from soil and clay by a dithionitecitrate system buffered with sodium bicarbonate. In: Clays and Clay Minerals. Proc. 7th Conf. Natl. Acad. Sci. Natl. Res. Council Publ. pp.317-327.

Nayak, A.K., Chinchmalatpure, A.R., Rao, G.G. and Verma, A.K. 2006. Swell-shrink potential of Vertisol in relation to clay content and exchangeable sodium under different ionic environment. *J. Indian Soc. Soil Sci.* **54**: 1-5.

Pal, D.K., Bhattacharyya, T., Ray, S.K., Chandran, P., Srivastava, P., Durge, S.L., Bhuse, S.R., 2006b. Significance of soil modifiers (Ca-zeolites and gypsum) in naturally degraded Vertisols of the Peninsular India in redefining the sodic soils. *Geoderma.* **136**: 210-228.

Peng, X., Horn, R., Smucker, A., 2007. Pore shrinkage dependency of inorganic and organic soils on wetting and drying cycles. *Soil Sci. Soc. Am. J.* **71(4)** : 1095-1104.

Piper, C.S. 1950. Soil and Plant Analysis (Reprint of original 1942 Edn. published by Inter science Published Inc. NY) The University of Adelaide, Australia pp. 368.

Qi, G., Michel, J.C., Bovin, P. and Charpentier, S., 2011. A laboratory device for continual measurement of water retention and shrink-swell properties during drying-wetting cycles. *Hort. Sci.* **46(9)** : 1298-1302.

Reeve, M.J., Hall, D.G.M. and Bullock, P. 1980. The effect of soil composition and environmental factors on the shrinkage of some clayey British soils. *Eur. J. Soil Sci.* **31(3)**: 429-442.

Richard, G.C. and Mitchell, J.K. 1968. Influence of temperature variation on soil behavior. *ASCE J. Soil Mech. Found. Div.* **94 (3)**: 609-734.

Richard, L.A. 1954. Diagnosis and Improvement of Saline and Alkali Soils, USDA Agric. Handbook 60, U.S. Govt. Printing Office, Washington, D.C. pp 160.

Rimmer, D.L. and Greenland, D.J. 1976. Effects of calcium carbonates on the swelling behavior of soil clay. *Eur. J. Soil Sci.* **27** : 129-139.

Ross, G.J. 1978. Relationships of specific surface areas and clay content to shrink–swell potential of soils having different clay mineralogical compositions. *Can. J. Soil Sci.* **58** : 159– 166.

Satyavathi, P.L.A., Balpande, S.S., Reddy, M.S., 2014. Water characteristics of some shrink-swell soils as influenced by clay and exchangeable cation. *Clay Res.* **26 (1-2)**: 23-31.

Schaffer, W.M. and Singer, M.J. 1976. A new method for measuring shrink-swell potential using soil paste. *Soil Sci. Soc. Am. J.* **40** : 805-806.

Shabtai, I.A., Shenker, M., Edeto, W.L., Warburg, A. and Ben-Hur, M. 2014. Effects of land use on structure and hydraulic properties of Vertisols containing a sodic horizon in northern Ethiopia. *Soil Tillage Res.* **136** : 19–27.

Sharply, A.N. 1989. Relationship between soil potassium forms and mineralogy. *Soil Sci. Soc. Am. J.* **52** : 1023-1028.

Shirsath, S.K., Bhattacharyya, T., Pal, D.K., 2000. Minimum threshold value of smectite for vertic properties. *Aust. J. Soil Res.* **38** : 189-201.

Simon, J.J., Oosterhuis, L. and Renaeau, R.B. 1987. Comparison of shrink-swell potential of seven Ultisols and one Alfisols using two different COLE techniques. *Soil Sci.* **143 (1)**: 50-55.

Smith, C.W., Hadas, A., Dan, J. and Koyumdijsky, H., 1985. Shrinkage and atterberg limits in relation to other properties of principle soil types of Israel. *Geoderma.* **35** : 47-65.

Soil Survey Staff, 1995. Soil Survey Manual. USDA, Handbook 18, U.S. Government Printing Office, Washington, DC.

Soil Survey Staff, 1999. Soil taxonomy: A basic system of soil classification for making and interpreting soil surveys, 2nd ed. Agriculture Handbook No. 436, SCS-USDA. US Govt. Printing Office, Washington, D.C. pp.857.

Soil Survey Staff, 2014. Keys to soil taxonomy, 12th edition (USDA-NRCS), pp.360.

Spark, D. L. 2002. Dynamics of K in soils and their role in management of K nutrition. In Potassium for sustainable crop productions. Proc. Intern. Symp. On role of potassium in nutrient management for sustainable crop production in India. Potash Research Institute of India, Gurgaon, Haryana, pp. 79-101.

SPSS, 2011. Statistical Package for Social Science (Release 20.0 version, 2011) Armonk, NY: IBM Corp.

Suguru, P. M. 2015. Effects of magnesium on cation selectivity and structural stability in prominent Vertisols of Karnataka .*Fungal Genom Biol.* **5 (1)** : 121.

Thakur, P. B. 2007. Relation between carbon content exchangeable cations and shrink-swell behavior of selected black soils. M.Sc. (LRM) Thesis Dr. Punjabrao Deshmukh Krishi Vidyapeeth, Akola pp. 85 (Unpublished).

Thomas, P.J., Baker, J.C. and Zelazny, L.W. 2000. An expansive soil index for predicting shrink–swell potential. *Soil Sci. Soc. Am. J.* **64** : 264-268.

Wilding, L.P., Williams, D., Miller, W.L., Cook, T. and Eswaran, H. 1990. Close interval spatial variability of Vertisols: A case study in Texas, in: Kimble, J.M. (Eds.), Characterization, Classification and Utilization of Cold Aridisols and Vertisols, Proc. 6th Int. Soil Correlation Meeting. USDA Soil Conservation Service, National Soil Survey Center, Lincoln, NE p. 232–247.

Yule, D.F. and Ritechie, J.T. 1980. Soil shrinkage relationship of Texas Vertisols; I. Small cores. *Soil Sci. Soc. Am. J.* **44** : 1291-1295.

(Received February, 2017; Accepted May, 2017)

ACKNOWLEDGEMENT

I grate fully acknowledge the help received from the followings scientists /Professors who reviewed the manuscripts for 2016 issue.

1. Dr Padikkal Chandran
2. Dr Sanjay Ray
3. Dr Goutam Goswami
4. Dr Siddhartha Mukhopadhyay
5. Dr K.M Manjaiah

INSTRUCTIONS FOR CONTRIBUTORS

CLAY RESEARCH is the official publication ofTHE CLAY MINERALS SOCIETY OF INDIA and is published twice a year, in June and December. The Journal undertakes to publish articles of interest to the international community of clay scientists, and will cover the subject areas of mineralogy, geology and geochemistry, crystallography, physical and colloid chemistry, physics, ceramics, civil and petroleum engineering and soil science.

The Journal is reviewed in *Chemical Abstracts, MineralogicalAbstracts, and Soils and Fertilizers.*

Paper (in English) should be submitted to the Editor, Clay Research **"The Clay Minerals Society of India"** Division of Soil Science and Agricultural Chemistry, l.A.R.l., New Delhi-I to 012. E-mail: samar_I953@yahoo.com. At least one of the authors should be member of THE CLAY MINERALS SOCIETY OF INDIA. Submission is an undertaking that the manuscript has not been published or submitted for publication elsewhere.

Manuscripts should not exceed sixteen typed (double spaced) pages including tables and illustrations. **The original and two copies oftext and illustrations should be submitted.**

Form Manusciprts should be typewritten, double spaced on white paper, with wide margins. Intending contributors should consult a recent issue of CLAY RESEARCH for the standard format and style. The manuscript should have the sections ABSTRACT, introductory portion (untitled), MATERIALS AND METHODS, RESULTS and DISCUSSION and REFERENCES.

Title page should contain manuscript title, full name(s) of author(s), address (es) of the institution(s) of the author(s), a short running title not exceeding 60 characters including spaces, footnotes if any to the title, and complete mailing address of the person to whom communications should be sent.

Abstract should be a condensation of the ideas and results of the paper. It should not exceed 25'0 words. Do not make reference to the literature in the abstract.

Tables should have the simplest possible column headings. Type each table on a separate page; indicate location in the text by marking in the margin of text page.

Figures should be self-illustrative, drawn with black India ink on tracing paper or white Board. The lattering should be large enough to permit size reduction to one Journal page column width (about 7.0 cm) without sacrificing legibility. **The original tracing should be submitted**. The size of the drawing should not exceed 24 × 17 cm. Give the numbered legend on a separate sheet, not on the figure itself. Data available in the tables should not be duplicated in the form of illustrations. Indicate the location of the figure in the text by marking in the margin of the page.

Photographs should be in the form of glossy prints with strong contrast. In photomicrographs, the scale in micron or other suitable unit should be drawn on the print. Give the numbered legend on a separate sheet. Indicate the location of the photograph in the text by making in the margin of the text page.

References should be cited in the text by the name(s) of author(s) if two or less, and year of publication. If there are more than two authors, give the name ofthe first author followed by *'et al'* and year. Full references giving author(s) and initial(s), year, title of paper, (journal, volume, number if paged separately), first and last pages should be listed alphabetically at the end of the paper. Journal title should be abbreviated in accordance with the World List of Scientific Periodicals and its sequences. Examples are

Grim, R.E., Bray, R.H. and Bradley, W.R. 1937. The mica in argillaceous sediments. *Am. Miner.* **22**:813-829.

Brindley, G.W. 1961. Chlorite minerals. In *(G.* Brown, Ed.) *The X-ray Identification and Crystal Structures of Clay Minerals,* Mineralogical Society, London, pp.242-296.

Theng, B.K.G. 1974. *The Chemistry of Clay Organic Reactions,* Adam. Hilger, London, 343 pp.

Review Every manuscript submitted to CLAY RESEARCH is independently reviewed by one or more referees. Acceptance or rejection of a manuscript is the responsibility of the Editor.

Reprints No free reprints are supplied to authors. Order for priced reprints should be sent when required by the Editor.

Clay Research

Vol. 35 **December 2016** **No. 2**

CONTENTS

Printed at : Cambridge Printing Works, New Delhi-1100028. (Mobile : 9811860113)